FINE SEDIMENT TRANSPORT NEAR CORAL REEFS ISLANDS IN THE SINGAPORE STRAIT

Baiq Dian Zoelaeha

Delft University of Technology

June 2010

The Erasmus Mundus MSc Coastal and Marine Engineering and Management is an integrated programme organized by five European partner institutions, coordinated by Delft University of Technology (TU Delft). The joint study programme of 120 ECTS credits (two years full-time) has been obtained at three of the five CoMEM partner institutions:

• Norges Teknisk- Naturvitenskapelige Universitet (NTNU) Trondheim, Norway
• Technische Universiteit (TU) Delft, The Netherlands
• City University London, Great Britain
• Universitat Politècnica de Catalunya (UPC), Barcelona, Spain
• University of Southampton, Southampton, Great Britain

The first year consists of the first and second semesters of 30 ECTS each, spent at NTNU, Trondheim and Delft University of Technology respectively.

The second year allows for specialization in three subjects and during the third semester courses are taken with a focus on advanced topics in the selected area of specialization:

• Engineering
• Management
• Environment
In the fourth and final semester an MSc project and thesis have to be completed.

The two year CoMEM programme leads to three officially recognized MSc diploma certificates. These will be issued by the three universities which have been attended by the student. The transcripts issued with the MSc Diploma Certificate of each university include grades/marks for each subject. A complete overview of subjects and ECTS credits is included in the Diploma Supplement, as received from the CoMEM coordinating university, Delft University of Technology (TU Delft).

Information regarding the CoMEM programme can be obtained from the programme coordinator and director

Prof. Dr. Ir. Marcel J.F. Stive
Delft University of Technology
Faculty of Civil Engineering and geosciences
P.O. Box 5048
2600 GA Delft
The Netherlands

DELFT UNIVERSITY OF TECHNOLOGY

FACULTY OF CIVIL ENGINEERING AND GEOSCIENCE

SECTION OF HYDRAULIC ENGINEERING

DEPARTMENT OF COASTAL ENGINEERING

Fine sediment transport near coral reefs islands in the Singapore Strait

Baiq Dian Zoelaeha

Graduation committee

Prof.dr.ir. M.J.F. Stive (Chairman, Delft University of Technology)

Dr.ir. J.C. Winterwerp (Hydraulic Engineering, Delft University of Technology/Deltares)

Dr.D.S. Van Maren (River Engineering, Delft University of Technology/Deltares

Acknowledgements

This study was carried out as part of the SDWA' Marine and Coastal Research Program "Large Scale Sediment Transport and Turbidity in the Singapore' Coastal Water"

I would like to thank the committee members; Prof. Dr.ir. Marcel Stive, Dr.ir. J.S Winterwerp and Dr. D.S. van Maren, for their valued input and critique to this thesis. Thanks especially to Deltares for providing place to work and to the maritime sediment project SDWA for access to project data for this thesis.

To my families, despite being far away, your encouragement and support has helped me very much, especially, to my beloved husband for believing in and supporting me to pursue higher education.

My fellow CoMEM 2008-2010 graduates, Serene, Huong, Quyen, Pandu, Bashar, Karunya, Anna, Danielle, Claudia, Jose, Rahman, Sarah, Mahtab, Nancy, Jimena, Badri, Claudio, Mehmet, and Wenjun, thank you for your friendship, humor and encouragement. It has been wonderful and great experiences to know you all over the past few years. Your friendships always made me feel accepted and live as Erasmus student would not be the same without you all.

To fellow Indonesian student associations in Delft, Southampton and Trondheim, thank you for support and help when I first came to those cities. I am grateful for all information and support while I adjusted to new places and make me feel like I was with my own family.

Finally, many thanks to Prof. Marcel Stive and the other hard working CoMEM staff in the NTNU (Trondheim) and Univ. Southampton (Southampton), whose vision for CoMEM program has provided this life-changing educational experience in Europe.

Baiq Dian Zoealeha

Delft, June 2010

Specially dedicate to:

My late grandfather

H. Lalu Djunaidi

My beloved parents

H.Lalu Sunarya and Hj. Baiq Susiawaty

My dearest husband

H. Lalu Abdurrahman, Lc

My dearest families

Iyus, Habib, Diah, Lutfi, Ali and baby Fahima

Abstract

The objective of this study is to determine large scale of fine sediment transport near coral reefs islands in the Singapore Strait. Coral reefs in the Singapore Strait face great pressure due to high sedimentation and turbidity, which cause decreasing of light penetration and of environment quality for the coral growth. Sedimentation and high level of turbidity are caused by large scale of dredging and land reclamations in the Singapore.

The location of Singapore Strait between two major water systems, leads to complex tidal system of the strait. Tidal elevation is predominantly semidiurnal while current velocity is diurnal. Field data from several tidal stations and offshore observation points are utilized in order to analysis large scale of fine sediment transport. The representative of time series from each observation point during the southwest and northeast monsoon were selected based on the data availability and quality.

Seasonal variation of current velocity shows eastward dominant flow during the SW monsoon and westward dominant flow during the NE monsoon. Residual flow plays more roles in the fine sediment transport than tidal asymmetry. Average residual flow ranges from 0.1 to 0.3 m/s with the peak 0.8 m/s in January. Wave action does not show significant impact to resuspension of fine sediment in deep water, but considerably cause fine sediment to resuspend at near surface. A turbidity level near coral reef islands corresponds to the fine sediment concentrations variation. High turbidity event occurs at all observation points and far from optimal level for coral growth. High turbidity event occurs more than weeks which is likely caused by resuspension of large sediment supply by strong currents.

Keywords: fine sediment, residual transport, tidal asymmetry, residual flow, turbidity

Table of Content

List of Figures

List of Tables

1 Introduction

1.1 Background study

Singapore's coral reefs are very attractive to the public because they can be seen from the shoreline without entering the waters and are located near the city. However, over the last half-century land reclamation and large scale dredging has increased the sedimentation and turbidity in the Singapore water threatening the sustainability of coral reefs (Chou, 2006). Despite the losses, there are more than 250 species of hard and stony corals from 55 genera, which provide habitat for more than 120 reef fish species from 30 families (Hamid and Lee, 2009). Most of remaining existing coral reefs can still be found at the southern islands of Singapore. Coral reef should be protected considering the important roles of coral reefs to marine ecosystem.

Coral reefs adjacent to the densely populated and heavily developed main island of Singapore have been subjected to increased sediment load over the past 50 years, mainly due to reclamations and dredging activities (Chia et al., 1988). The sources of sediment input into the water of the southern islands of Singapore are multiple, frequents, mobile and extend several kilometers from Singapore, such as river discharge, seabed dredging, and the dumping of dredged spoils (Chou, 1994, Dikou and van Woesik, 2006).

Increased sedimentation and suspended sediments smothers live corals, which require more energy expenditure to remove overlies sediment. Furthermore, turbidity reduces light penetration for photosynthesis process and coral growth, compresses biotic zones, and reduces hard coral species richness (Dikou and van Woesik, 2006). Sedimentation measurements have been conducted in several monitoring points in Singapore. For example the sedimentation rates (predominantly sand with some silt) around P. Semakau are 10 to 90 mg/cm^2/day, which corresponds to 7 to 65 cm/year (Chou et al., 2004). Turbidity was not measured until recent years and therefore the apparent increase turbidity is mainly based on qualitative or semi quantitative description. Chou and Chia (1991) stated that water visibility was still approximately 10 m depth around the Southern Islands until as recently as the early 1960s, and that the extensive land reclamation project have resulted very high levels of sedimentation often reducing the visibility to less than 2 m in a clear day. The present day suspended sediment concentration is typically between 5 and 20 mg/l along the west coast of the southern islands of Singapore with water depth of approximately 4 m was based on the survey of 6 islands for one year period and at the depth of 4 m, the present study measured an 85% reduction in light (Dikou and van Woesik, 2006).

While research has been carried out around the coral reefs island, there is still a gap in understanding the processes responsible for the increased turbidity and its effect on coral reefs in the Singapore Strait. In particular, detemining the mechanisms responsible for increased turbidity is not straightforward because there is often very limited data on

sediment pathways, bed sediment composistion, sediment concentration and hydrodynamics; historic data to compare present-day with natural conditions are often scarce. Moreover, the physical behavior of the sediment mixture in the water column such as concentration, settling, segregation, erosion, and resuspension is still insufficiently understood.

1.2   Problem analysis

Over the last 20 years of rapid coastal development in the Singapore straits, sedimentation and increased turbidity have become a major issue in the areas. The fine suspended sediment concentration mainly caused by extensive and large scale dredging and land reclamation, in which it increases turbidity level in the Singapore Strait, in particular close to the coral islands. Moreover, high levels of turbidity reduced the light penetration which is useful and important for coral reefs growth. Therefore, a study on fine suspended sediment transport and turbidity near the coral reefs island is important to determine driven mechanisms that responsible for the increased turbidity.

1.3   Thesis objectives

The objectives of the research are to determine the fine sediment transport around the coral reefs of Singapore. Several important research questions are:

1. What are large-scale sediment transport mechanisms and what is relative influence of tides, waves, residual flows and river discharge
2. What are local resuspension mechanisms and what is the relative influence of tides, waves, and residual flow to resuspend the sediment,
3. What is the typical duration and level in high turbidity event?

1.4   Research boundaries

There is several research boundaries applied in this study in order to support the analyze process, such as:
1. The focus of this study is on fine sediment because this mainly contributes to the turbidity. Hence, only fine suspended sediment and not bed load transport will be considered
2. The hydrodynamic and sediment dynamic are analyzed based on available data.

2   Theoretical background of fine sediment transport

Considering the impact of high turbidity and sedimentation to coral reefs community, it is important to understand the behavior of fine sediment transport and turbidity around the coral reefs environment. There have been numbers of extensive studies on the fine sediment transport which were based on the local and regional area for example fine sediment transport on specific estuaries and bays (Van de Kreeke and Robaczewska, 1993, Wolanski et al., 2008, Storlazzi et al., 2009, Wolanski et al., 1996, Wolanski et al., 2005, Hoitink, 2004, Hoitink and Hoekstra, 2003, de Jonge, 1992). This chapter will discuss general theoretical background of fine sediment transport and turbidity from various studies.

2.1   Introduction

In general, the suspended load is mainly composed of fine sediment with particle size ranging between 1 and 10 μm (quartz, feldspar, clay minerals) and aggregates with a size up to 100 μm (Dronkers, 1986). The classification of sediment based on the grain size is shown in the Table 1. Fine sediment transport behavior is different from the coarser sediment transport, which is influenced by the cohesive properties, for example consolidation and flocculation, and related time lag effects. Fine sediment can also be maintained in suspension even at small current velocities and the concentration of fine suspended sediment is limited by the availability of the erodible bottom material, for instance, by consolidation or by the presence of an overlying coarse sediment layer (Dronkers, 1986).

One of the important properties of sediment determines the fate of fine sediment transport is the settling velocity. The settling velocity for non cohesive and cohesive sediment is affected by different factors. For non cohesive sediment, such as sand, the settling velocity is a function of particles' size, diameters, shape and the water viscosity, and can be determined straightforwardly with great accuracy. For cohesive sediments, the settling velocity will be influenced by the tendency of sediment to form flocs of varying size and composed of clay properties, silt, fine sand, organic material and water (Winterwerp et al., 2006). Moreover, the settling velocity of cohesive sediment also influenced by the concentration of particles, salinity, temperature and organic material (Van Rijn, 1993).

Table 1. Grain size scale American Geophysical Union

Class Name	Millimeters	Micrometers	Phi Values
Boulders	> 256		< -8
Cobbles	256 - 64		-8 to -6
Gravel	64 - 2		-6 to -1
Very coarse sand	2.0 - 1.0	2000 - 1000	-1 to 0
Coarse sand	1.0 - 0.50	1000 - 500	0 to +1
Medium sand	0.50 - 0.25	500 - 250	+1 to +2
Fine sand	0.25 - 0.125	250 - 125	+2 to +3
Very fine sand	0.125 - 0.062	125 - 62	+3 to +4
Coarse silt	0.062 - 0.031	62 - 31	+4 to +5
Medium silt	0.031 - 0.016	31 - 16	+5 to +6
Fine silt	0.016 - 0.008	16 - 8	+6 to +7
Very fine silt	0.008 - 0.004	8 - 4	+7 to +8
Coarse clay	0.004 - 0.0020	4 - 2	+8 to +9
Medium clay	0.0020 - 0.0010	2 - 1	+9 to +10
Fine clay	0.0010 - 0.0050	1 - 0.5	+10 to +11
Very fine clay	0.0005 - 0.00024	0.5 - 0.25	+11 to +12
Colloids	< 0.0024	< 0.24	> +12

Source: (Van Rijn, 1993)

2.2   Residual transport mechanisms

The basic transport process in tidal flow has been explained in van Rijn (Van Rijn, 1993) as shown in the Figure 2-1.
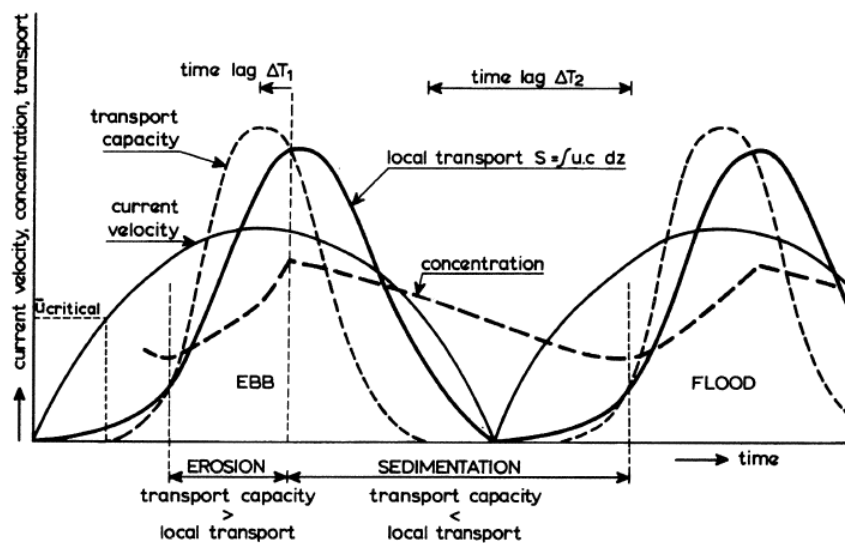
Figure 2-1. Sediment transport mechanism under tidal action

Sediment particles become suspension when the current velocity exceeds a critical value. In accelerating flow there is always a net vertical upward sediment particle due to turbulence-related diffusive process, which continues as long as the sediment transport capacity exceeds the actual transport rate. Moreover, the term of time lag also should be considered in the sediment transport driven by the tide. Time lag (T1) is the period between the moment maximum flow and the moment of equal transport capacity and actual transport rate. After this latter moment there is a net downward sediment transport because settling dominates yielding depth the settling process can continue during the slack water period giving a large time lag (T2) which is defined as the period between a zero transport capacity and the start of a new erosion cycle. In addition, the suspended sediment transport during decelerating flow is larger than the accelerating flow.

Sediment may be transported in a preferential direction due to an asymmetry in ebb and flood flow velocities and/or water levels, and lag effects. Asymmetries in ebb and flood flow velocities may be caused by residual flow (a net flow velocity in addition to the oscillating tidal currents) or by tidal asymmetry. An asymmetry in tidal currents is here called maximum flow asymmetry. An asymmetry in water levels is usually tidally driven, and an asymmetry known as slack tide asymmetry may contribute to a net transport of sediment as well. These processes will be elaborated below.

2.2.1 Tidal asymmetry

The important component of the effect of tide in the sediment transport is the tidal asymmetry. Tidal asymmetry has been a major subject in a lot of literature related to sediment transport in the marine environment. The tidal asymmetry is a difference between the maximum current velocities occurring during flood and ebb (Dronkers, 1986). Tidal asymmetry may generate a difference between maximum ebb and flood flow velocities, which is defined as a maximum flow velocity. This asymmetry generally produces a transport in the direction of maximum flow (van Maren et al., 2004). In addition, tidal asymmetry may generate a difference in duration of ebb and flood slack tide, which is important in fine sediment transport. During the period around slack tide, part of the fine sediment load settles, in particular the aggregates with a size on the order of 100 µm and larger (Dronkers, 1986, Postma, 1961).

Studies on the importance of tidal asymmetry in the transport and accumulation of sediment in the tidal system appears from studies on tidal rivers and estuaries (Dronkers, 1986, Van de Kreeke and Robaczewska, 1993); tidal inlet (Aubrey and Speer, 1985); and tidal basin (Postma, 1961). These studies focused on residual transport caused by tidal asymmetry in the semidiurnal regime, particularly that of the M_2-M_4 interaction. Moreover, tidal asymmetry generated by astronomical tides in absence of shallow water effect has been investigated in the specific diurnal regime, which is relatively less common (Hoitink et al., 2003). The interaction of tidal constituents, in particular the K1, O1, and M2, give an

asymmetrical periodic flow patterns, with the largest peak velocities persistently in the same direction.

2.2.1.1 Maximum flow asymmetry in semi diurnal regime

To describe the influence of tidal asymmetry on the sediment transport, there are two types of transport should be considered, which are bed load transport and suspended load transport. Based on study by Van de Kreeke and Robaczewska on tide-induced residual transport of coarse sediment (1993), the contribution of M_2 and its overtides (M_4, M_6) and the residual flow velocity (M0) is the major driven force for long term mean bed load transport. By considering a single fundamental harmonic, for example M_2, the asymmetry in the velocity curve as a result of the presence of overtides. The development of tidal asymmetry is described in the Figure 2-2.
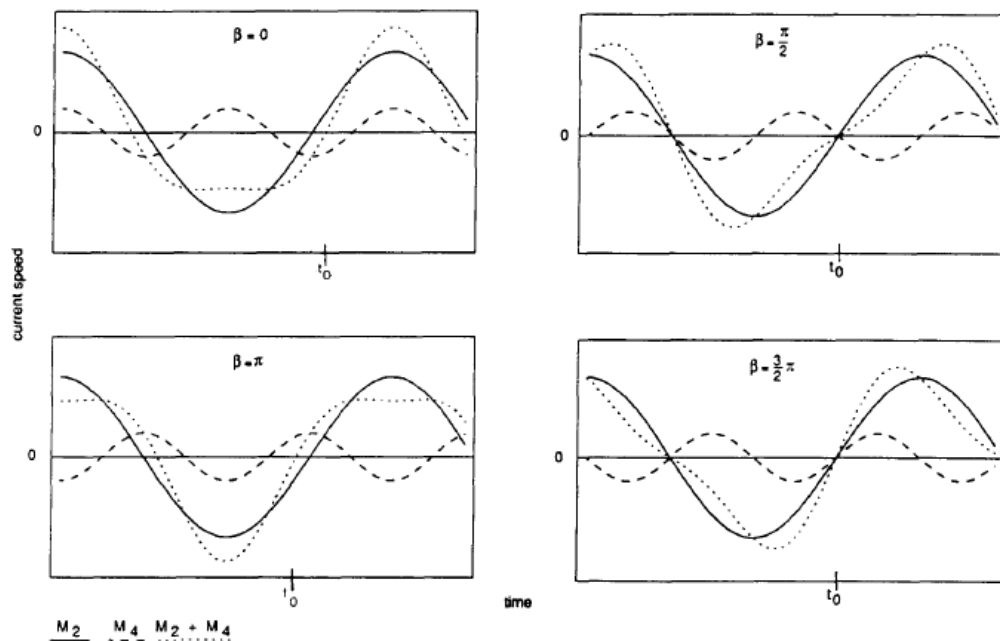
Figure 2-2. M_2 and M_4 tidal constituents,

source: (Van de Kreeke and Robaczewska, 1993)

It can be seen from Fig. 2-2, flood dominance is found for $-\pi/2 < \beta < \pi/2$ and ebb dominance for $\pi/2 < \beta < 3\pi/2$. Flow reversal from flood to ebb (high water slack) is of shorter duration than low water slack for $0 < \beta < \pi$ and of longer duration from $\pi < \beta < 2\pi$. Furthermore, in order to determine the effect of the tidal current variations on the sediment transport, they assume a simple sediment transport formula:

$$s = fu^3 \hspace{10em} \text{Eq 1}$$

where f is a function of the sediment and fluid characteristic and u is given by:

$$u(t) = u_0 + \hat{u}\cos(\omega t) + \sum_n u_n \cos(\omega_n t - \varphi_n) \hspace{6em} \text{Eq 2}$$

Where:

u = flow velocity, t =time , u_0= residual flow velocity , $\hat{u}$=amplitude of the M2 tidal current , ω = angular frequency of the M2 tide , u_n= amplitude of other tidal current constituents, ω_n= angular frequency of other tidal constituents , ϕ_n= phase of other tidal constituents.

The long term (several months) tide induced bed load flux is then can be described as:

$$\frac{\bar{s}}{f\hat{u}^3} = \frac{3}{2}\frac{u_0}{\hat{u}} + \frac{3}{4}\frac{u_{M4}}{\hat{u}}cos\beta + \frac{3}{42}\frac{u_{M4}}{\hat{u}}\frac{u_{M4}}{\hat{u}}cos(\beta - \gamma)$$ Eq 3

where:

β = phase of the M$_4$ tidal current relative to the M$_2$ tidal current (φ_{M4}-$2\varphi_{M2}$)

γ = phase of the M6 tidal current relative to the M2 tidal current (φ_{M6}-$3\varphi_{M2}$)

The expression showed in the Eq.3 proof that the relative amplitudes of the tidal constituents are important to the residual transport. The relative phases of the overtides strongly influence both the direction (ebb or flood dominant) and the magnitude of the transport. The net residual transport due to interaction between M$_2$ and M$_4$ is illustrated in the Fig. 2-3.
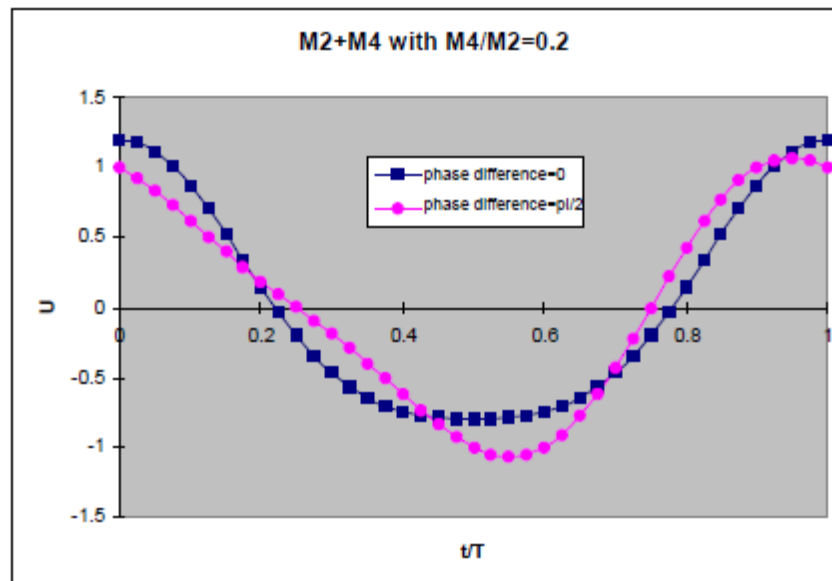
Figure 2-3. Net residual transport due to M$_2$+M$_4$

Source: (Bosboom.J and Stive, 2010)

Furthermore, the transport mechanisms illustrated by Eq.3 also can be applied to the suspended transport (Wang, 2008). In the case of fine sediment, the suspended sediment transport not only depends on the local instantaneous flow velocity but also on the flow conditions upstream. The time scales of erosion and sedimentation become important, a

characteristic that causes as essential difference in the tidal dynamics of fine sediment (silt) compare to coarse sediment (sand). For sand, this time scale is an order of magnitude smaller than the tidal period, whereas for fine sediment the time scale are of similar order. The fine suspended sediment occurs due to relaxation effect in the sediment concentration.

$$u = \sin(\omega t) + 0.5 \sin(\omega t) \qquad\qquad \text{Eq 4}$$

$$c_e \propto u^2 \qquad\qquad \text{Eq 5}$$

$$\frac{\partial c}{\partial t} = \frac{c_e - c}{T_a} \qquad\qquad \text{Eq 6}$$

$$s \propto uc \qquad\qquad \text{Eq 7}$$

Where: u = current velocity, c_e = equilibrium concentration, c = suspended sediment concentration, T_a = time scale for which the suspended concentration approaches the equilibrium concentration.

In terms of sediment characteristic, the effect of tidal asymmetry is varying. For fine sediment, the asymmetry between the duration of slack water at high and low tide is considered to be a key factor controlling the net direction of transport (Postma, 1961, Dronkers, 1986), while for coarser sediment (sand), the tidal asymmetry in the peak velocities becomes important in particular the ratio of the amplitude of the vertical tide of the M_2 and M_4 overtide and their phase difference $2\_M_2\_M_4$ (Van de Kreeke and Robaczewska, 1993). If the phase difference (of the vertical tide) is positive, the transport in the estuary is flood-dominated. In the case of estuaries where the tidal range is large relative to water depth, considerable asymmetry can occur in the tidal curve because the effect of friction increases with the decreasing water depth. As a result, the high water travels more quickly into the estuary than the low water, the tidal curve becoming saw-toothed in shape, with a quick rise at the beginning of the flood tide as a slow fall towards low water.

2.2.1.2 *Maximum flow asymmetry in diurnal regime*

Another approach to compute residual transport of sediment due to tidal asymmetry in relation to astronomical tides constituents has been carried out by Hoitink et al, (2003). Considering the tide constituent of K_1, O_1, and M_2, the angular frequency of each astronomical tidal constituent can be expressed in terms of sums and difference of six basic frequencies $\omega 1 - \omega 6$,

$$\omega = i_a \omega_1 + i_b \omega_2 + i_c \omega_3 + i_d \omega_4 + i_e \omega_5 + i_f \omega_6 \qquad\qquad \text{Eq 8}$$

where ω_N refers to the angular frequency of constituent N with unit rad/s and coefficients i_a to i_f are small integers known as Doodson numbers (Hoitink et al., 2003). A flow component, $\hat{u}$, composed of three constituents of K1, O1 and M2 is expressed as:

$$\hat{u} = A_{K1}\cos\big((\omega_1 + \omega_1)t - \phi_{K1}\big) + A_{O1}\cos\big((\omega_1 - \omega_1)t - \phi_{O1}\big) + A_{M2}\cos(2\omega_1 t - \phi_{M2}),$$
Eq 9

where A_N and φ_N refers to the amplitude and phase of constituent N, respectively. The duration of spring neap cycle, T, coincided with the synodic of K1 and O1, which amount of 13.66 days.

By adopting the theory of Bagnold, relation between residual sediment transports can be derived. The equilibrium concentration of suspended sediment can be related to the depth mean flow velocity , *u*, as in (Groen, 1967):

$$c_e = k\bar{u}^p \qquad\qquad\qquad\qquad \text{Eq 10}$$

With c_e is equilibrium concentration, k is a constant of proportional and p is a constant power (p range between 2-3). Ignoring depth variation of *u* and *c*, the sediment transport rate S can be approximated as the product of $\bar{c}$ and $\bar{u}$. Under the assumption of p = 2, the analytical expression for the residual sediment transport is (Hoitink and Hoekstra, 2003):

$$S = \frac{3}{2}kA_{K1}A_{O1}A_{M2}F \qquad\qquad\qquad\qquad \text{Eq 11}$$

where *S* = residual transport (m³), *F* = attenuation factor within the range of -1 and 1.

The residual transport rate depends mainly on the relative phased difference and the flow amplitudes of K_1, O_1 and M_2.

2.2.1.3 Slack tide asymmetry

For fine sediment transport the asymmetry of duration between high water slack and low water slack plays important roles. If the high water slack (HW, flow reversal from flood to ebb) is longer than the low water slack (LWS, flow reversal from ebb to flood), a strong sedimentation occurs around HWS, whereas in the intial ebb phase only little material is in suspension. Later in the ebb period more fine sediment is suspended. Around LWS part of this sediment settles, but not too much because of the short slack water duration. When flood current increases in strength, immediately a relatively large amount of suspended sediment material is transported. Subsequently, the suspended concentration increases even further. Average over flood, the concentration of suspended sediment is therefore larger than during ebb.

2.2.2   Lag effect

Another important issue of tide effect on the sediment transport is lag effect. In general there are four cases lag effects which have been reviewed extensively by Dyer (1995).

1. Settling lag: around slack water, when the flow is no longer able to keep in suspension, the sediment will settle. However, settling takes time, as a result of which the sediment is transported beyond points where the flow falls below its transport capacity. Sediment settling velocity and local water depth governs the magnitude of the settling lag. As a result sediment is transported from areas with high flow velocity to areas with low flow velocity. Moreover Dronkers (1986) emphasized the time interval during which sediment particles can settle at slack water and remain on the bottom until resuspended and concluded that the magnitude and direction of the residual sediment flux is mainly determined by the current velocities around low water and high water slack. Depositional periods at high water generally exceed those at low water.

2. Scour lag: following slack water, the flow accelerates and will re-erode the sediment deposited during the slack water. However, flow velocities (bed shear strength) to re-erode sediment deposits are larger in general than the flow velocity to keep the sediment suspension. Hence, bed strength, erosion rate and vertical mixing time govern the magnitude of scour lag.

3. A threshold lag is produced by the presence of a threshold for sediment transport. When coupled to an asymmetry in the tidal currents, sediment movement can take place for longer time on one phase of the current compared with another. As an example, in a tidal cycle with an intense short flood current and a long ebb current velocity, the duration of movement on the ebb tide will decrease more rapidly than that on the flood with increase in the threshold of sediment movement.

4. Erosion lag is produced by an increase of the critical erosion shear stress with depth, because of consolidation. Consequently, once the surface layers have been eroded, the new surface materials requires high velocities to cause movement. With increasing bed shear stress on the flood tide the critical erosion shear stress at the bed surface becomes exceeded and erosion progressively proceeds into the sediment at a rate that is governed by the variation of bed shear with time, as well as the variation of erosion shear stress with depth, and the sediment is suspended.

2.2.3   Residual flow

Residual flows can be produced by wind drag on the sea surface or driven by lateral density gradients due to non uniform salinity or temperature distributions or by the tidal flow itself. It is non-linear interactions of the oscillating tidal streams, leading to residual flows. Tidally driven residuals are important because they are persistent features, linked to the local

bottom or coastal topography, fluctuating only with the strength of the semidiurnal tides over the regular spring neap cycle (Robinson, 1983). Although the tidally induced residual flows are considerably weaker than storm driven residual flows, they can contribute more significantly to overall long-term distribution and transport of water properties that the stronger, but intermittent and directionally inconsistent wind driven flows.

The magnitude of tidally residual flow is dependent on the phase coupling between the horizontal and the vertical tide. If u is the tidal current velocity in 1D channel, h is the mean water depth and η is the water surface elevation above mean sea level, and let u and η be given by:

$$\eta = a\sin(\omega t - kx) \text{ and } u = \hat{u}\sin(\omega t - kx) \hspace{2cm} \text{Eq 12}$$

Then tidal residual flux is given by :

$$q_{Res} = \hat{u}(h + a)\frac{1}{T}\int_0^T \sin(\omega t - kx - \varphi)\sin(\omega t - kx)\,dt = \frac{1}{2}\hat{u}\,(h + a)cos\varphi \hspace{1cm} \text{Eq 13}$$

If the horizontal tide (u) and the vertical tide (η) are 90° out of phase (φ =π/2), there is no flux, but if the they are more or less in phase ($\varphi \approx 0$), there can be a considerable residual current. The relation between the tidal cycle and residual flow is described in the Fig.2-4.
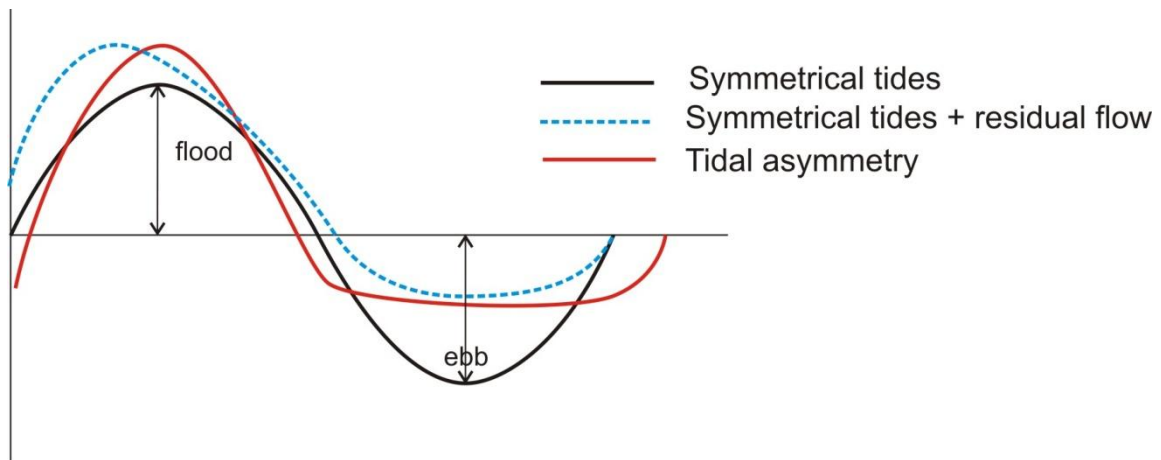
Figure 2-4. Schematic tidal symmetry and residual flow

During symmetrical tide, the flood current velocity and the ebb current velocity is the same, however, tidal asymmetry occurs when the flood current velocity is higher and its duration is shorter than the ebb duration. Meanwhile, because the ebb flow needs more time to retreat causes the duration of ebb flow is longer and the current velocity is lower. The combination of tidal asymmetry and residual flow control the net sediment transport.

For bathymetry induced circulation, the residual flow tends to be ebb directed in the deeper part, whereas it tends to be flood directed in the shallower part. Geometry induced circulations occurs where the tidal flow is obstructed by a structure such as a breakwater.

Illustrations of both types of circulation are shown in the Fig. 2-5 (Bosboom.J and Stive, 2010).

Figure 2-5. Geometry induced (left) and bathymetry induced (right) circulation

2.2.4 Monsoon current

Wind driven flow in the tropical area is relatively regular because of the cycles of monsoons and trade winds. The tropical regions around equator, such as near Indonesian archipelago and Malaysian peninsula, are under strong influence of the Asian monsoon system. The seasonal winds reverse semi annually between northern winter (November-March) and summer (May-September). The general monsoon current pattern during both season are show in the Fig. 2-6 and Fig 2-7. During the northern winter monsoon, a westward flowing North Equatorial current (NEC) is present in both the Indian and the South China Sea. The NEC pushes water mass up north along the east coast of India into Bay of Bengal creating a huge clockwise gyre north of 5 N, while in the South China Sea an anticlockwise eddy is formed due to the penetration of NEC and current from the Yellow sea. The eddy, together with the NE monsoon winds creates a strong current along the east coast of the Malaysian Peninsula and Sumatera down to the Java Sea. During the northern summer monsoon as shown in the Figure 5, the South Equatorial Current (SWC) is strengthening. This strong current originates from the Java Sea goes through the Strait of Kalimantan into the South China Sea and is strengthened further along the coast of Sumatera and the Malaysian Peninsula by summer monsoon winds.

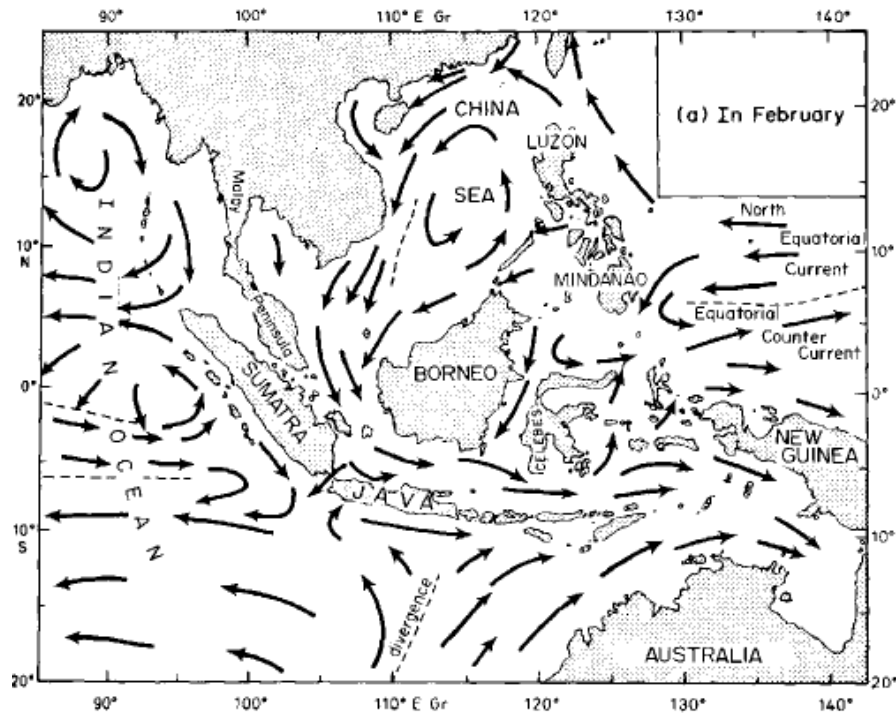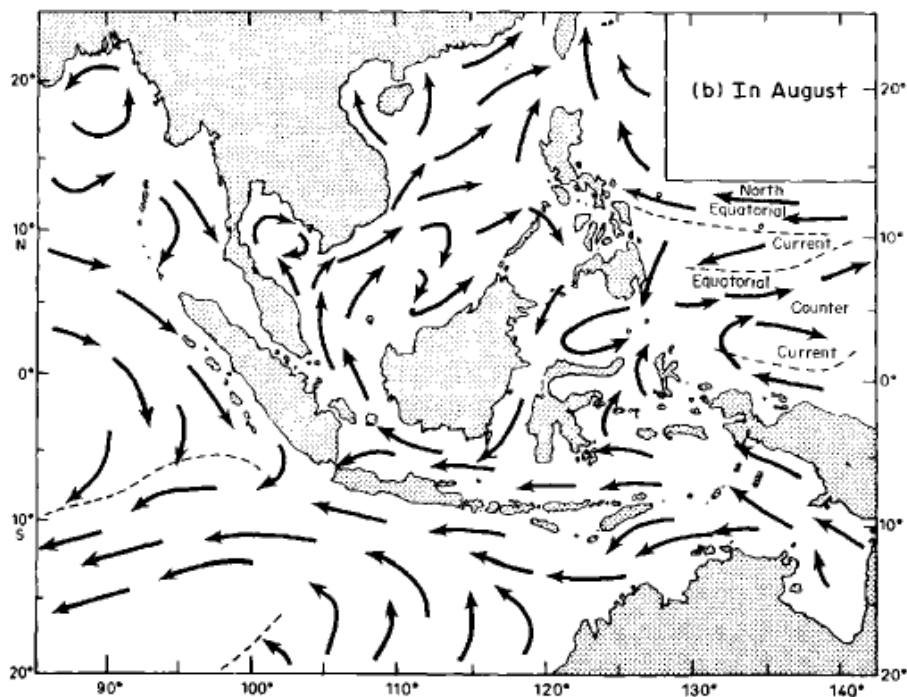Figure 2-6. Current pattern during North-East Monsoon

Figure 2-7. Current pattern during South-West Monsoon

2.3 Wave induced resuspension

Wave induced sediment transport processes are related to the velocities generated by high and low frequency wave phenomena. Net onshore transport is dominant in non breaking wave condition, whereas net offshore transport is dominant in breaking wave condition. In

the case of wave propagate near islands and coral reef, wave transformation on coral reef has been comprehensively explained by Massel (1996) and Gourlay (1994). Steeper waves start to break early as the distance from shallow reef edge, and their breaking intensity is higher than that of smaller waves. Waves at low steepness lose their stability their stability closer to the reef edge and dissipate energy mostly on the reef platform, where water depth is in the order of 2 m (Hoitink, 2003). Wave action is largest at the surface, which may be associated with a large capacity to mobilize sediments. Moreover, the small, short-period waves are only able to resuspense sediment in the shallow and exposed part of environment. The threshold at which sediment motion is activated by waves is (Hoitink and Hoekstra, 2003):

$$h = 10H_s \hspace{4cm} \text{Eq 14}$$

where h = depth, H_s = wave height

2.4 The impact of turbidity to visibility

Turbidity refers to an optical property of liquid that measures the scattering and/or absorption of light due to material suspended in the solution. Turbidity responds to variation of the high and low water. In general case, at high water, the concentration during the ebb tide the maximum is moved seaward and by entrainment of sediment from the bed, the concentration increase.

The impact of sedimentation and turbidity on coral reef is well documented. The response of coral communities towards sediment load depends on the size of the sediment particles, the intensity of the load, the rate of sediment dispersal, the presence of other stressors, the geographic setting, and on the initial coral composition (Dikou and van Woesik, 2006). Fabricius (2005) noted that the level and duration of turbidity and sedimentation play significant factor in the ecological response of both individual corals and coral reef ecosystem. Furthermore, the important factor contributing to the level of degradation caused by a given stressor is level of exposure, which is a function of concentration and residence time, both of which are influenced by hydrodynamic processes. Sedimentation has been linked to profound changes in coral population's structures such as altered size frequencies, declining mean colony size, altered growth forms, and reduces growth and survival (Woolfe and Larcombe, 1999). The light reduction due to turbidity which is direct function of particle concentration and water depth caused changing in the coral community structures and life forms, reduced species richness, reduced growth, increase mucus production and compressed depth zonation (Fabricius, 2005, Woolfe and Larcombe, 1999).

3 Description of Study Area

This chapter discusses the physical description of the Strait of Singapore, which includes the hydrodynamic characteristic, coastal seabed and landform, coral reefs status and environmental condition required by coral reefs in Singapore.

3.1 Physical hydrodynamic characteristics

3.1.1 Location, boundaries and bathymetry

The Singapore Strait is bounded by Singapore's and Malaysia's southern coast on one side and the northern coasts of Indonesia's Riau Island. It connects the Malacca strait on the west and the South China Sea on the east. Additionally, the Malacca and Singapore Strait are connected to the Java Sea through Selat Durian, Selat Combol and Selat Riau and several other minor straits between islands (Chan et al., 2006).

Bathymetry of the strait and surrounding coastal areas influences the current and the circulation pattern in the strait. Water depth in the northern part of the Singapore Island, where it is connected with the Johor strait and the South China Sea, is approximately from 10 to 20 m along the centre of the strait and the width along the Johor strait varies from about 0.5 to 2 km including the tidal flats on the both sides of the straits. On the southern part of the Singapore coast, the narrowest part of the Strait is about 5 km and between Singapore and Batam Island, the range is about 5 km to 15 km. The water depth is generally less than 50 m from the southern end of the Malacca Strait to the South China Sea, however, in a small area just off the coast of the south east of St John Island, the water depth is more than 100 m. The bathymetry of the Singapore Strait is shown in the Figure 3-1.

3.1.2 Tide, monsoon, and currents

The monsoon winds are generated by a combination of trade winds and the seasonal variation of the position of the sun. Near the equator, the trade winds generate a persistent system of the easterly winds and the equatorial pressure trough moves according to the position of the sun and generating a north-south component of the winds direction. The climate of Singapore is characterized by two monsoons, south-west (SW) monsoon from May to October, and north-east monsoon (NE) from November to March. During the wetter NE monsoon, it brings more rain then sunshine and there is a net transport of water from the South China Sea to the Singapore Strait. Conversely, during the SW monsoon, water from the Java Sea and the Malacca Strait is transported through the Singapore Strait (Dikou and van Woesik, 2006).
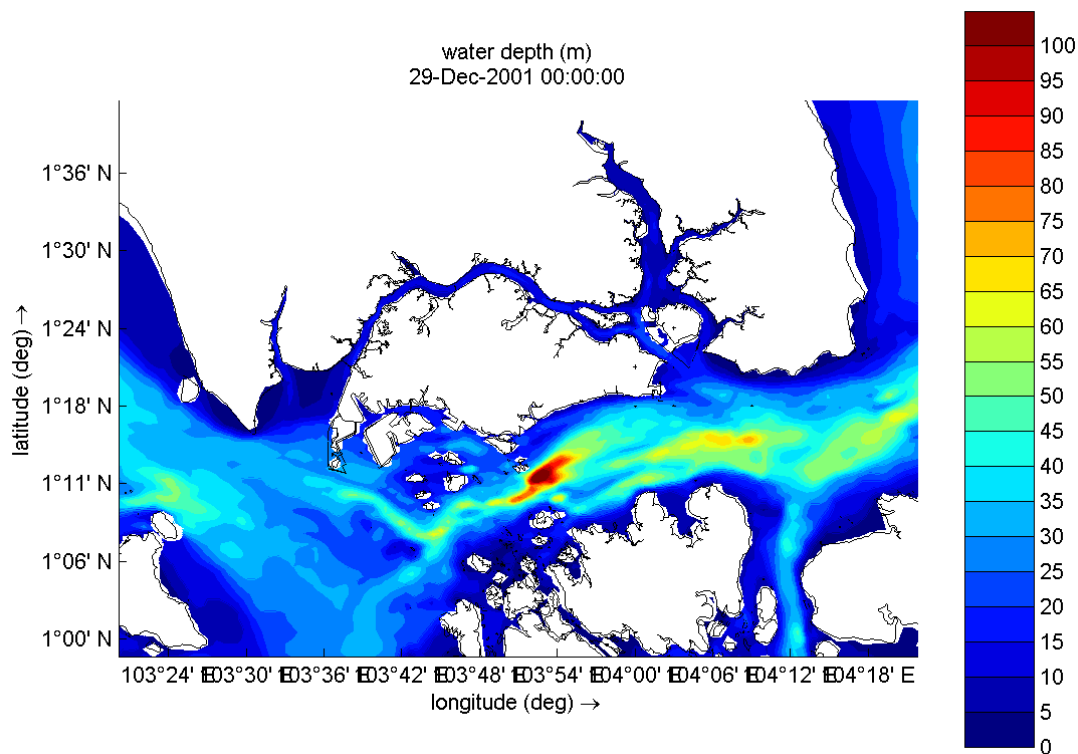
Figure 3-1. Bathymetry of the Singapore Strait

Owing to the nature of Singapore Strait as a conduit of South China Sea and the India Ocean, it is logically acceptable that the tides in the strait are generated by tidal waves from those ocean and sea. However, those characteristics of tides are different. Tides are dominated by semi diurnal tides and diurnal tides in the South China Sea, while in the Indian Ocean tides are dominated by a semi diurnal frequency. Semi diurnal tides in the South China Sea mainly consist of the principal solar component S_2 and the principal lunar component M_2, while diurnal oscillations is associated with the moon declination (K_1 and O_1) (Chen et al., 2005). A list of the amplitudes of the six major tidal harmonics observed at four sites across the Malacca strait and the Singapore Strait is shown in the Table 2. Moreover, near the western part of the strait two tidal meet and causes a complicated tidal pattern along the strait. On average, the spring range at the western end is about 2.87 m and twice as much as that at the eastern end. The neap range across the strait is about 40% to half of the spring range (Chen et al, 2005). Tidal range is 2.5-3.0 m during spring and 0.7-1.2 m during neap. Tidal stream velocities vary from 0.5-1.0 ms-1 in the open waters of the Strait of Singapore to as much as 1.5-2.0 ms-1 in constricted channels between islands (Wong, 1985). Non tidal current arising from prevailing winds can attain a maximum speed of 0.4 m/s during the North-East monsoon.

Table 2. Tidal constituent in the Singapore Strait

Harmonic Components	One Fathom Bank (middle of Malacca Strait)	Iyu Kecil west end of Strait of Singapore	Raffles Lighthouse	Horsburgh Lighthouse (east end of the Strait of Singapore)
S1	3.71	3.89	2.09	0.64
K1	11.48	26.49	27.03	26.65
O1	9.91	25.92	25.20	27.92
M2	117.59	94.41	82.97	56.46
S2	58.34	43.31	36.85	19.06
N2	22.25	17.34	15.25	11.39

Source: Chen et al, 2005

Singapore Strait is located in an exceptionally sharp transition zone where dominantly diurnal tides (between Sumatera and Borneo) change into semi diurnal tides (between Sumatera and Malaysia) within distance of only 100 km. This transition is due to increasing the amplitude of the M_2 amplitude and decreasing in diurnal amplitude, especially in the Singapore Strait. As a result, this strong gradient generates strong tidal currents in the Strait. In addition, tidal wave of each tidal constituent is the combination of a progressive wave and a standing wave. Progressive wave have maximum current at high water and low water (lagging the water by 180°) and their magnitude increase with the wave amplitude. Therefore, they do not exist near amphidromic points where the water levels variation is low. Standing waves, however, have maximum tidal current at amphidormic points, with current lagging tidal the water levels with 90°. As a result, sharp transition in tidal regimes may generate tidal current in the Singapore strait which strongly deviate from local water levels (Deltares et al., 2008).

In terms of ocean circulation pattern in the strait, it is likely to be accepted that the circulation in the strait is influenced by circulation in the South China Sea, the Indian Ocean and the Java Sea. Moreover, apart from the Asian monsoon influence, the North Equator Current (NEC) and the South Equator Current (SEC) also have strong effect on the Strait current (Pang and Tkalich, 2003). During the winter monsoon, the South China Sea eddy accumulates water up at the eastern entrance of the strait while the northern Indian Ocean eddy pulls water down at the other end of the Malacca strait. As a result, an east-west hydrodynamic pressure gradient is created, which produces a net drift from east to west in the strait. In contrast, during summer monsoon, the strong eastward current in the northern Indian Ocean pushes water level up at the northwest entrance of the Malacca Strait while the northward current passing the South China Sea entrance of the Singapore Strait drags the water level down which lead to the net drift from west to east (Pang and Tkalich, 2003, Chen et al., 2005)

Several attempts have been carried out to model hydrodynamic in the Singapore Straits and the surrounding water (Chen et al., 2005, Zhang and Gin, 2000, Pang and Tkalich, 2003).

Some of recent efforts include boundary fitted grid model and full three dimensional models (Pang and Tkalich, 2003, Chen et al., 2005). From these studies, strong tidal current are apparent throughout the strait and in general currents are typically less than 2 ms^{-1} in most part of the Singapore Strait except in the narrow channel between St John's Island and Pulau Lengkana. Easterly flows in the Singapore Strait are usually associated with the rising tide and remain eastward flowing when tidal elevation in the strait dips slightly before rising again. On the other hand, westward flows in the Singapore Strait are associated with the decreasing tides (Chan et al., 2006). Although wind driven current are dominant in the open areas such as the South China Sea, the influence of the wind on the currents in the Singapore and Malacca Straits are less significant compared to the tidal forcing. Residual ocean current related to the monsoons occurs and they are an order of magnitude smaller than the peak tidal currents (Chan et al., 2006).

Modeling on the circulation pattern in the Singapore Strait estimates the net volume transport during two monsoon seasons (Chen et al., 2005). The transport change dramatically with season and fluctuated between about 1.5 x 10^5 m^3/s eastward and 2.5 x 10^5 m^3/s westward during the heights of monsoon seasons in December and June, to minimum close to 0 during the inter monsoon seasons around March and September. The net volume transport across the strait is controlled by the pressure gradient created by monsoonal mean sea level difference, tidal range difference, and the topography.

3.1.3 Winds and Wave

In general, wind speed around Singapore is low. The maximum wind speed is 8m/s during the Northeast monsoon. As consequently, the wave fetch length is short and the direction of maximum fetch length rarely coincide with the direction of the strongest winds.

Location of Singapore provides low wave energy environment. Wave energy is dissipated through obstruction and refraction bay the shallow water, islands and reefs. Wong (1985) reported that wave measurement, which was carried out at Bedok, showed almost 55 % of Hs (significant wave height) to be 0.2-0.4 m during the northeast monsoon and 0.1-0.2 m during the rest of the recording period. The maximum-recorded eave height was 1.1 m with a period of 3 seconds. Higher value was recorded occur at five kilometers east of Changi during the monsoon due to refraction of swell from the South China Sea, which resulted in Hs was 1-1.25 m and the period 6-7 seconds.

3.1.4 River discharge

River discharge is a significant source of sediment. The largest rivers drain to the Singapore water is the Johor River which flowing into Johor estuary. In comparison, there are several small rivers system which is not more than 20 km flow from Singapore island, for example the Punggol, the Sungei Buloh, the Sungei Kranji, the Sungei Seletar, the Sungei Seranggoon flow into the Johor Strait while the Sungei Kallang drains into the Singapore Strait (Chia et

al., 1988). Moreover, the Johor River long term average discharge is 37.5 m^3/s, vary from 30 m^3/s in February 70 m^3/s to around in December and October (see Fig. 3-2). Therefore it can be assumed that other smaller rivers have a similar seasonal variation, but lower discharge.

Sediment load of small rivers in Singapore Islands is rarely available; however sediment concentration of Johor River can be used as comparison. It is reported that average concentration of the Johor is 79.8 mg/l (with minimum and maximum tabulated values of 35 mg/l and 164 mg/l) (Najah et al., 2009). A study on run off from a small urban catchment in the Skudai river shows maximum concentrations during high energy events up to 1 g/l (Nazahijah et al., 2007).
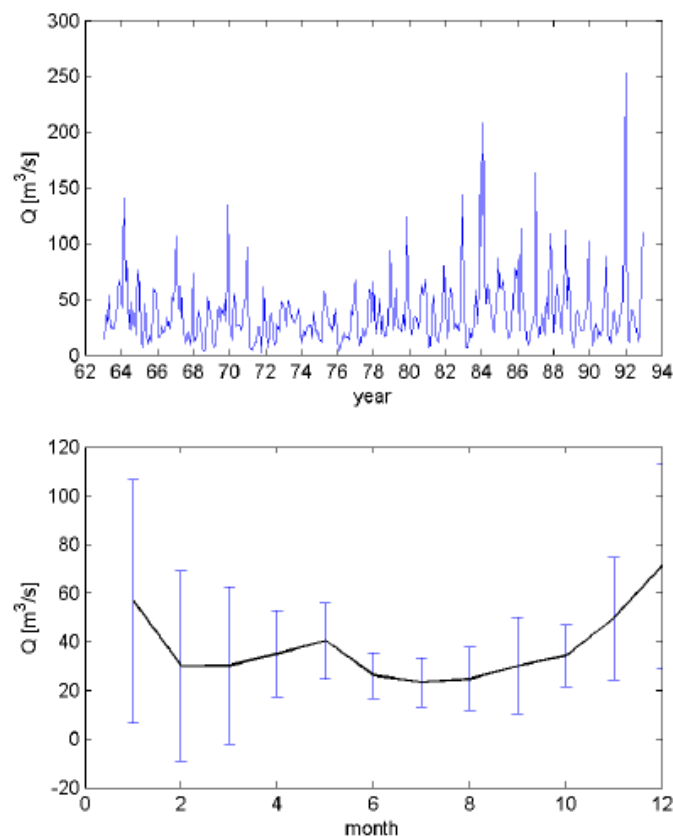
Figure 3-2. Discharge of the Johor River near Rantau Panjang (catchment area of 1130 km^2), annual time series (top) and monthly averages, with standard deviation (bottom). Source from West-Malaysian drainage and irrigation

3.2 Coastal sediment

3.2.1 The origin of marine sediment

The studies on the coastal area of Singapore (Chia et al., 1988, Bird et al., 2006, Bird et al., 2007, Hesp et al., 1998, Hilton and Chou, 1999, Tan et al., 2003) explain the origin and the characteristic of marine sediment of the Singpaore Island. The soil on the Singapore Island is

generally classified into six major formations known as Kallang formation, Old Alluvium, Jurong formation, Bukit Timah Granite, Gombak Norite and Sahajat formation (PWD (1976) in Tan et al, (Tan et al., 2003). The Kallang Formation which covers most of the coastal plain and immediate offshore zone is a recent deposit and consists of soil of marine and alluvial including sands, silts, clays and peats (Tan et al., 2003, Chia et al., 1988). A study by Bird et al (2006) on the sediments of the Singapore Strait which was based on the Quaternary geology and detailed bathymetry, suggest that a marine connection between the Indian Ocean and the South China Sea through the strait may not have existed until the last interglacial period. Moreover, the earliest marine sediment consists of lower marine clay and upper marine clay which are main constituent of the Kallang Formation (PWD (1976, in (Tan et al., 2003). Lower marine clay is homogenous green grey clay with occasional macroscopic fragments of shell and organic detritus while the upper marine clay is similar in characteristics to the lower marine clay and was deposited after the most recent flooding of the strait (Bird et al., 2006).

Chia et al (1988) divided the Kallang formation into five subtypes, which includes the marine member, the alluvial member, the transitional member, the littoral member and the reef member. The marine member consists of blue grey silty clay with sandy, peaty, and shelly layers while the Alluvial member consist of pebble beds, sands mans peats. The transitional member is found in the river mouth consist of a series of unconsolidated black organic muds up to 13 m thick. The Littoral member forms coastal beach sands and gravels, offshore sands and tidal sand banks, mostly found in the Southern Islands and in shoals south of P.Tekong, east of P. Ubin and P.Seletar. Finally, the active reef members are found in the Southern and Southern-western Islands.

Seabed configuration of the Singapore waters is highly irregular due to numerous islands and shoals. Although most of the coastal waters are not more than 30 m deep, there is a small area deeper which is found at the south east of St John Island with water depths reach more than 100 m (Chia et al., 1988, Chan et al., 2006). The seafloor is covered with unconsolidated sand and mud which were deposited after the sea level rose, however, the mud is absent along the channel where the velocity of tidal current is high (Chia et al., 1988). Moreover, beside the river discharge, which bring land based sediment source into the strait, the seafloor is considered to be source of sediment as well, in particular fine sand and mud. Accumulation of mud around Singapore Strait can be seen in the Figure 3-3. Fluvial sediment supply is probably coming from the south west coast of Malaysia Peninsula; however, the origin of the mud is still unclear. In addition, seabed dredging activities and the dumping of dredging material during the development of Tuas Island and Jurong Islands

Figure 3-3. Sediment supply around Singapore Strait (Source: (SDWA, 2010)

3.2.2 Land reclamation and dredging

During rapid development in the Singapore and pressure to meet high demand of area for port and properties, land reclamation and dredging activities has increased sedimentation around Singapore water. Overview of land reclamation and dredging activities in Singapore is showed in the Figure 3-4. Land reclamation has transformed most of intertidal areas of the estuaries and reclaimed mangroves forest in the coastal areas which is preventing the accumulation of fine sediment. Not only the alteration of mangrove forest changes the land use of the area but also changes the sediment balance between terrestrial sediment from river discharge and increase the turbidity in the marine waters. The mangroves that remain in Singapore are located in isolated patches on the sheltered coast of the main islands and on the offshore island of Pulau Tekong and Pulau Ubin to the northeast, and Pulau Pawai and Sengan to the south (Bird et al., 2004). A large reforestation programs was initiated in the late 1990s at Pulau Semakau to compensate the loss of mangrove due to the construction of containment of seawall for landfill site. Reforestation was carried out at both, north and south of the connection to replace the loss and the growth of seedlings was vigorous, which make the effort can be considered successful.

Extensive dredging has caused the environmental impact in regard of resuspension of sediment during dredging. The environmental impact of dredging has been studied in relation to the heavy metal level in the marine sediment and changes in sediment organic content and adverse effect on the resident community structure of the environment Moreover, the quality of marine sediment in the coastal water of Singapore are contaminated by the pollution and emission from boat, increasing shipping activities, pollutants release from industrial sources and dredging (Nayar et al., 2004a). The pollutant includes heavy metals; persistent organic pollutants and oil related industries. The levels of

heavy metals in marine sediment was largely dependent on sediment particle size that fine sediment have a larger surface area which allows heavy metals and other contaminant to be adsorbed easily (Chia et al., 1988, Nayar et al., 2004b).
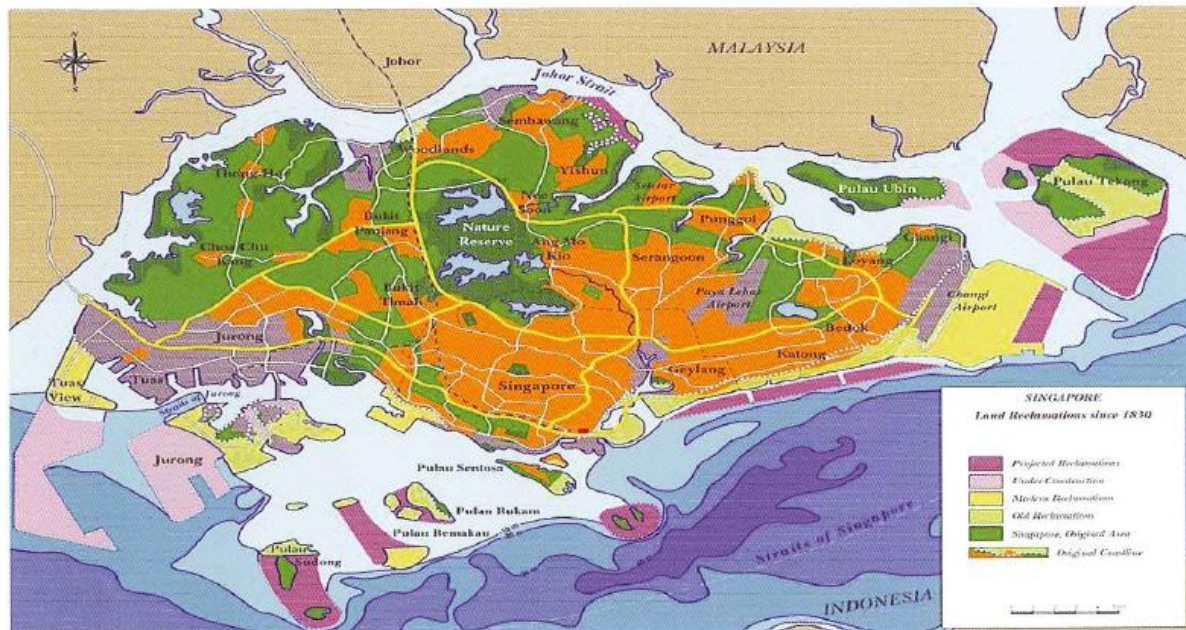

Figure 3-4. Overview of land reclamation is Singapore since 1830 (source: (SDWA, 2010)

3.3 Coral reefs system in the Singapore Strait

3.3.1 Status of coral reefs

The coastal water of Singapore provide excellent conditions for the marine life due to its location in the tropical areas which offers relatively constant water temperature and frequent fresh ocean flow from both the South China Sea and the Malacca Strait. Coral, seagrass and mangrove habitats have been found to be relatively rich in Singapore. There are 250 of coral species which is included in 55 genera. For seagrass habitat, 12 species out of 57 known species are found in Singapore where as 24 out of 54 of mangrove species have been found in the Singapore (Hamid and Lee, 2009). These numbers show the high diversity of marine habitats is relatively small area as Singapore and the importance of marine habitat conservation in Singapore.

Many investigations were carried out on Singapore reefs and a monitoring program since 1987 indicates the response of reefs to the diversity of impacts. It is estimated that 60% of reefs have been lot to reclamation and the remaining are exposed mainly to sediment impact (Chou, 2006, Chou et al., 2008). Regular dredging of shipping channels and dumping of the spoils further offshore ass to the suspended sediment load generated from land reclamation. Direct shipping impact come from waves generated by the vessels, particularly the high speed ferries. Increased wave energy from the high speed ferries exposed the reef crest and the flats. Moreover recent observation shows that direct physical damage of

shallow reefs by construction or transport barges, which destroy considerable tracts if reefs (Chou et al., 2008).

Rapid light attenuation of the water column has prevented coral survival below 6 m depth. Growth is now restricted to the upper reef slope and the crests support the best reef development. Table 3 indicated overall decline in live coral cover as well as a reduction in the abundance of reef associated invertebrates, although a few reef sites showed improvement, for example at Cyrene site 1 and 2, where the percentage of live coral cover increase to 21.1 % and 25.7%.

Table 3. Percentage of temporal variation in live coral cover found on 11 reef sites

Site	Temporal variation in live coral cover (%) at reef crest	
	1986-89	2000-03
Cyrene (site 1)	10.2	21.1
Cyrene (site 2)	20.1	25.7
Hantu West (site 1)	41.5	38.8
Hantu West (site 2)	70.4	13.6
Pulau Hantu (site 1)	31.4	8.6
Pulau Hantu (site 2)	49.1	46.8
Pulau semakau (site 1)	26.1	23.4
Pulau Semakau (site 2)	51.8	21.4
Raffles Lighthouse (site 1)	76.6	56.7
Raffles Ligjthouse (site 2)	76.1	48.8
Terumbu Bukom		46
Terumbu Banyan		38
Lazarus Island		14
Labrador beach		26

Source:(Chou, 2006)

The location of coral reefs islands in Singapore is shown in the 3-5. It can be seen that most the coral islands are located in the south part of the strait. Most of Singapore coral reef is fringing reef and some of them are patches reefs. The islands with fringing reefs range in elevation from 3 to 8.5 m above MSL, while the patch reefs attain levels to approximate mean low water neap (Hilton and Chou, 1999).

3.3.2 Tolerance limits of sedimentation for corals in the Singapore Strait

In the case of Singapore coral reefs, the initial tolerance limits of sedimentation for corals have been establish based upon a number of experiences in the similar dredging project in the South East Asia region (Doorn-Groen, 2007). The tolerance of coral to suspended sediment is about 10 mg/l which based on the study in Hongkong water. However, extensive monitoring data from multiple projects in Singapore has allowed the development of a coral tolerance matrix for excess suspended sediment which is shown in the Table 4. In the turbid environment around Singapore's water, low concentration sediment plumes in the surface of the water column are generally not visible if the excess concentration above

background does not exceed 5 mg/l (Doorn-Groen, 2007). The tolerance limits is useful to set the standard for future dredging activities and to lead most environmentally sound dredging activities.

Figure 3-5. Coral reefs islands in the Singapore Strait (Source: (Deltares et al., 2008)

Table 4. Coral reef tolerance level to suspended solid

Severity	Definition (excess concentration)
No Impact	Excess Suspended Sediment Concentration > 5 mg/l for less than 5% of the time
Slight Impact	Excess Suspended Sediment Concentration > 5 mg/l for less than 20% of the time Excess Suspended Sediment Concentration > 10 mg/l for less than 5% of the time
Minor Impact	Excess Suspended Sediment Concentration > 5 mg/l for more than 20% of the time Excess Suspended Sediment Concentration > 10 mg/l for less than 20% of the time
Moderate Impact	Excess Suspended Sediment Concentration > 10 mg/l for more than 20% of the time Excess Suspended Sediment Concentration > 25 mg/l for more than 5% of the time
Major Impact	Excess Suspended Sediment Concentration > 25 mg/l for more than 20% of the time Excess Suspended Sediment Concentration > 100 mg/l for more than 1% of the time

Source: (Doorn-Groen, 2007)

4 Data collection and processing

This chapter will discuss about the process of data collection and processing, including description of tidal station and sediment observation buoys.

4.1 Data collection

Tides data and sediment concentration are collected from several tidal station and offshore buoys around the Singapore Strait. Tides data ranges from 1996 to 2008 collected from 8 tidal stations with different time intervals 10 to 30 minutes recording, while data on sediment concentration and velocity range from 2002 and 2008 were obtained from 7 buoys. Location of tidal stations and offshore buoy is shown in the Fig 4-1. The amount of data on sediment concentration and current velocity vary from all buoys. Some buoys show irregular data that considered being non valid, for example extremely high concentration value and current velocity.
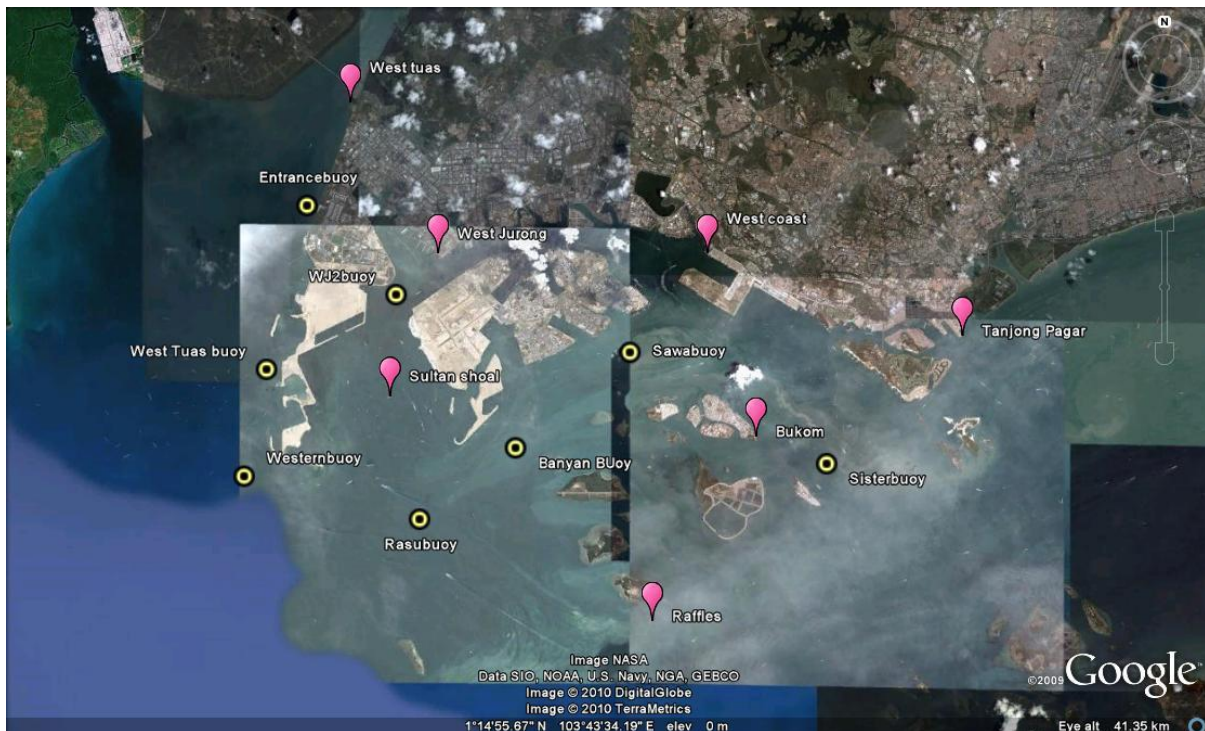

Figure 4-1. Location of tidal stations (yellow circle is offshore buoy, red is tidal station) (source: Google earth)

In terms of location of each observation point and tidal stations, the nearest observation points from fringing coral islands include Rasubuoy, Banyanbuoy, Sisterbuoy, Sawabuoys, Raffles tidal station, Bukom tidal station, and Sultan Shoal tidal station. However, in order to obtain broader understanding on fine sediment transport behavior in the strait, all data from other observation point also will be analyzed.

4.1.1 Tidal Stations

1. Bukom

Bukom tidal station is located at Pulao Bukom, one of coral reef islands in the Singapore Strait and is geographically located at latitude of 1°13'32.32"N and 103°46'42.52"E. Nowdays , P.Bukom is the site for the Shell's oil refinery and plants for manufacture of chemicals. Based on the reef monitoring in 2000, the percentage of dead coral with the sub crest less than 2,5 meter due to high turbidity and sedimentation reached to 46 %. Tidal data from this station was recorded from 1996 to 2008 with interval time 6 minute. The tides recorded from this station shows strong semidiurnal tide with the water level range from 0.5 to 3.5 during spring and 0.5 to 2.5 during neap.

2. Raffles light house

Raffles lighthouse is geographically located at 1° 9'36.29"N and 103°44'29.52"E. It is also located at the southern off-shore island of the Singapore, Pulau Setumu. Pulau Setumu is well known as best place to dive in Singapore for beautiful coral reefs and fish marine park. The tide water elevation is range between 0,2 to 3,5 m during spring and 0,2 to 2 m during neap.

3. West coast ferry terminal

West coast ferry terminal is situated geographically 1° 17' 30" North of the Equator and longitude (103.7619 degrees) 103° 45' 42" East. Tidal recorded from this station range from 1997 to 2008 and similar to other stations, it shows strong semidiurnal tide. The water level ranges from 0.2 to 3.3 m during spring and 1 to 2 m during neap. Shipyards are concentrated along this terminal which causes extensive port activities and maritime transportation.

4. West Jurong

West Jurong is located at 1°17'26.75"N and 103°39'54.92"E. West Jurong is busy terminal and one of important industrial area in Singapore. Tidal range in West Jurong is 0.3 to 3.5 m during spring and 1 to 2.5 m during neap.

5. Sultan shoal

Sultan shoal tidal station is located at 1°14'24.12"N and 103°38'53.18"E. Tidal range is between 0.3 to 3.5 m during spring and 1.2 to 2.5 m during neap.

6. West Tuas (Raffles marina)

West Tuas is important industrial area in the western part of Singapore. It was reclaimed since 1973 and nowadays, West Tuas is intended for port, residence area and heavy

industry. The tidal station is located geographically 1°20'39.94"N and 103°38'2.33"E. Tidal range between 0.3 to 3.3 m during spring and 1 to 2.5 m during neap.

A sample of tidal elevation observed in one of the tidal station is shown in the App.A.

4.1.2 Offshore Buoys

Offshore buoys are located around the Singapore Strait as shown in the Figure 4-1 . The range of data from these buoys is varying in term of availability and the accuracy. Six of buoys are placed as surface buoy while two of them are placed near the seabed. The summary of offshore buoy measurement is shown in the Table 5.

Sediment concentration and current velocities data from all observation points can be seen in the App. B and App. C. Although the measurement was conducted in considerably long period of time, not all data are reliable to be analyzed. This is because in some buoys, the data availability is limited and yield unreliable data as a result of instrumental and measurement errors or due to local man-induced disturbance, for example, at Rasubuoy and Banyanbuoy, the highest concentration recorded in 2002 is above 1000 mg/l, which is considered unrealistic. Sediment concentration data from the Westernbuoy are relatively low and the amount of data is less than others and only presents data from 2003 to 2004. Moreover, sediment concentration data from West Tuas buoy and W2J buoy have the longest time series, however, the instruments have been set up to detect certain maximum concentration which makes the maximum concentration is fixed. Data on velocity current was recorded in different depth which is useful to determine the vertical profile of the velocity in the strait. However, in some buoys, particularly at Westuas and W2J buoys, data on velocity current is limited compare to the concentration data from the same buoys. Therefore in these particular buoys, the relation between concentration and velocities is analyzed based on the available current velocity data.

For the purpose of data analysis, representative sediment concentration data are selected during specific time period in two seasonal monsoons. Concentration data from the selected time periods are considerably available from all observation points. For the Southwest monsoon (May-Sept), the selected time period is May, representing maximum residual flows during the SW monsoon. For the Northeast monsoon, the selected time period is November-December, representing strong NE monsoon residual flows. General description of the data quality from all observation point is explained as follows:

1. Banyan Buoy

    Data from Banyanbuoy is relatively poor because of the amount of data is limited and does not cover entire monthly periods. The representative time period for the SW monsoon is September, where data of sediment concentration and current velocity are

available and the variation during spring neap tide is clearly shown. However, the representative data for the NE monsoon is not available.

2. Rasubuoy

The amount of data from Rasubuoy is considerably covers all time periods. It can be distinguish between low concentration and concentration periods. The representative data for the SW monsoon is November, while data obtained in May represent the NE monsoons.

3. Sawabuoy

Data from Sawabuoy shows large difference in the level of concentration. Sediment concentration from March to May is very high, while during other time period, it is considerably low. The representative data for high concentration is taken from May which represents the SW monsoon, whereas data from November is selected to represent the NE monsoon. The cause of a large difference in the sediment concentration data is not clear.

4. Sisterbuoy

Data from Sisterbuoy shows long term similar values and tidally variation signal. To represent the SW monsoon, data from June is selected to represent the SW monsoon because part of data in May is missing. Data from November represents the NE monsoon and the concentration is relatively lower than that during the SW monsoon.

5. Westernbuoy

Data from the Westernbuoy is considerably poor because of the limited amount of data and does not show clear tidally signal. Therefore, data from Westernbuoy is not used for further analysis.

6. Westtuas

Data from relatively covers most of the time, however, there are many sudden variation of concentration in short time. The representative data from the SW is selected from half of May and June time period. Whereas for the NE monsoon, representative data is not available because of discontinuity of time series that it cannot provide a full spring neap cycle for the analysis. There are several gaps of the current velocity data that make difficulties in selecting the same time period for concentration and current velocity. The current velocity unit for this buoy is in m/s.

7. W2J

Data from W2J buoy shows some missing time series; in particular during March and September, however, it still can provide representative data from both SW and NE

monsoons. The selected time period of May and December are used in further analysis. Moreover, the unit for current velocity in this buoy is m/s, while in other buoy, the current unit id in cm/s.

Table 5. Summary of tidal measurement

Station name	Stncode	Lat (N) (deg min)	Long (E) (deg min)	Start date	Start time (hh:mm)	End date	End time (hh:mm)	Time resolution (min)
Bukom	Bk	01 13.5386	103 46.7087	20-nov-96	0:00	18-apr-08	8:00	6
Raffles	Rl	01 09.6048	103 44.4920	23-oct-96	21:18	18-apr-08	8:00	6
Sembawang	Se	01 27.8784	103 50.0517	4-nov-96	11:18	18-apr-08	8:06	6
Sultan shoal	Ss	01 14.4020	103 38.8864	19-nov-96	0:06	18-apr-08	8:00	6
Ferry terminal 1 (West coast)	Wc	01 17.5127	103 45.6713	3-apr-97	11:24	18-apr-08	8:12	6
West jurong	Wj	01 17.4458	103 39.9154	11-dec-96	13:18	18-apr-08	8:12	6
West tuas (raffles marina)	Wt	01 20.6656	103 38.0389	24-nov-96	0:06	18-apr-08	8:12	6

Table 6. Summary of sediment concentration measurement

No.	Name	Lat (N)	Long (E)	Deployment	Deployed On	Last data	Time interval (min)	Turbidity Measurement	No. Of Speed & direction measured	Speed Unit
1	Banyanbuoy	01-13.317	103-41.6-	Buoy	01-Feb-02	31-Oct-03	30	Yes	5	Cm/s
2	Westernbuoy	01-12.712	103-35.798	Buoy	05-Jan-03	30-Nov-03	30	Yes	5	Cm/s
3	Rasubuoy	01-11.796	103-39.549	Buoy	01-Jan-02	28-Nov-03	30	Yes	5	Cm/s
4	Sawabuoy	01-15.354	103-44.045	Buoy	01-Jan-02	30-Nov-03	30	Yes	5	Cm/s
5	Sisterbuoy	01-12.979	103-48.248	Buoy	05-Jul-02	30-Nov-03	30	Yes	5	Cm/s
6	Westtuas	01-14.991	103-36.277	Seabed	01-Nov-02	31-Mar-08	10	Yes	1	M/s
7	Wj2Buoy	01-16.585	103-39.047	Seabed	01-Jan-02	14-Mar-08	10	Yes	1	M/s

5   Data analysis and Result

Data analysis was carried out to determine large scale sediment transport mechanism and relative influence of tides, waves and residual flows as driven mechanism of fine sediment transport in the Singapore Strait. The concentration is plotted against the velocity current with the same time series which is included seasonal time series, the spring neap cycle and the 24 hours tidal cycle.

5.1.1   Seasonal variation tidal current velocity and residual flow

Location of the Singapore between two major water systems; the Malacca Strait and the South China Sea, results in the complex mixed tidal system. The interaction between the semidiurnal and diurnal tides in the narrow strait of Singapore causes strong tidal current o developed. Mixed tides system in Singapore Strait is dominated by semi diurnal tides; however, the diurnal tide dominates two times per year, alternating the dominance semidiurnal tides. This alteration is the result of the phase difference between the O1-K1 spring neap cycle (13.66 days) and M_2-S_2 spring neap tidal cycle (14.77 days), which resulting in a 182.62 days periods. This is exactly half a year time period which implies the variation of semidiurnal and diurnal dominance is constant through time. In addition, mixed tide environment produce dominant semidiurnal water level and dominant diurnal current velocity (see Fig. 5-1)

As can be seen from Figure 5-1, there is residual seasonal variation of current velocity along the strait. The maximum residual current velocity of 0.8 m/s occurs in January 2003, when the northeast moon was fully developed. During the SW monsoon (May-September), the residual flow direction dominated by eastward direction with relatively low current velocity (0.2 m/s-0.4 m/s). Whereas, during the NE monsoon (November-March), a reversal residual flow westward occurs at the strait as response to pressure gradient in the surrounding ocean. The residual flow velocity during NE monsoon is larger and stronger than residual flow during the SW monsoon, which is probably because the winds from the north east are stronger in the South China Sea. However, during the transition period, the flow directions show inconsistency, particularly in July 2003, the residual flow direction is relatively random towards east and west. High residual flow in the strait is probably generated by eddies caused by tide-topography interaction and by large scale of residual flow driven by monsoon currents. Zimmerman (1980) showed that vorticity produced by an oscillating current on irregular topography is partly transferred to a mean residual current. Considering the bathymetry of the Singapore Strait, it is likely that residual flow induced by irregular bathymetry combined with monsoon current produce high residual current in the Strait.

In order to determine the relative role of residual flow in the Singapore Strait, analysis on shorter time series will be carried out. In the next section, analysis of the tidally variation of sediment concentration during spring neap cycle and the 24 hours plotting will discussed.

The spring neap cycle is selected during two different seasonal monsoons in order to differentiate the relative effect of residual flow and tidal asymmetry to the fine sediment transport in the strait.
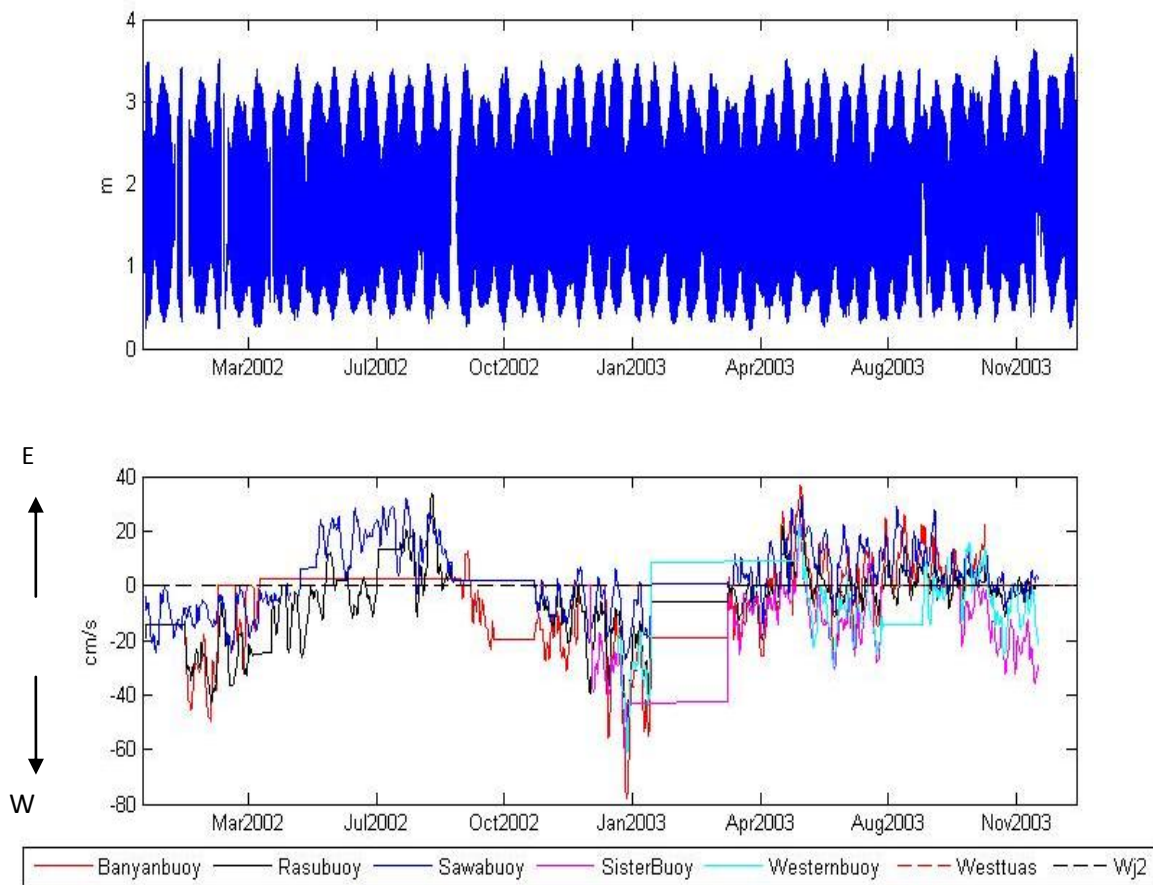

Figure 5-1. Residual flow measured from all offshore buoys (positive current velocity represents eastward direction)
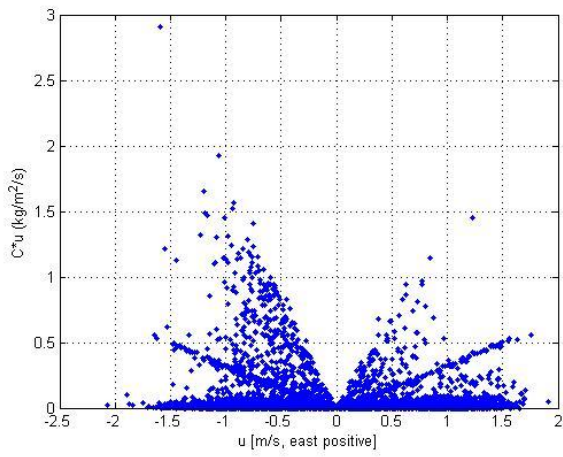
5.1.2 Sediment Flux

It is noted that sediment flux depends on the sediment concentration and the current velocities, which implies the current velocity direction influences the direction of advection of the suspended sediment. In idealized situation where there is no sediment pick up or settling, the advection of a suspended sediment concentration would produce the same concentration on rising and failing current. However, the entrainment of sediment from the bed produces an increasing concentration on the accelerating tides and settling lag causes the maximum concentration to lag the maximum velocity.

Sediment flux observed at 6 observation points is shown in the Figure 5-2. All time series of sediment flux is plotted against the major current velocity. The highest sediment flux occurs at Banyan Buoy, which reaches 1.5 kg/m^2/s and the lowest flux occurs at Westtuas. At

Banyanbuoy, sediment flux toward westward direction is relatively similar to eastward flux and the higher flux occurs in westward direction with flux of 2 kg/m^2/s. It can also be seen that there are more events of low flux occurs than events of high flux. Furthermore, sediment flux at Rasubuoy shows a significant symmetry of eastward and westward direction. However, compare to Banyanbuoy, sediment flux at Rasubuoy is lower due the level of concentration at Banyanbuoy is higher than at Rasubuoy.

At Sawabuoy, there are more flux to eastward direction than to westward direction, with maximum flux of 0.9 kg/m^2/s occurs during eastward flow. In contrast, sediment flux at Sisterbuoy is relatively symmetrical, although the high flux occurs during westward flow. Maximum sediment flux at Sisterbuoy is 0.2 kg/m^2/s while at Sawabuoy maximum flux is almost 1 kg/m^2/s. At Westtuas and W2J, sediment flux is considerably lower than other buoy as the concentration and the current velocity at these places are lower. However, it can be seen that dominant direction of the flux between these places is different. Westward flux direction dominates at Westuas, while eastward flux direction dominates at W2J.

Despite the difference of flux dominant direction showed in the Fig. 5-1, it is hard to conclude factor causing such differences. As sediment flux depends on the concentration and the current velocities, the availability of these data in the same amount is crucial to determine the trend on dominant flux direction. For observation points that have limited and unequal amount of data for entire months, it can produce significant difference of flux dominant direction, for example Banyanbuoy, Sawabuoy and Westtuas. For observation points with considerable amount of data for entire months, such as Rasubuoy and Siterbuoy, it will be easier to determine the dominant flux directions. Therefore, to get more understanding on the trend of sediment flux, further analysis of sediment flux during shorter time period will be carried out.
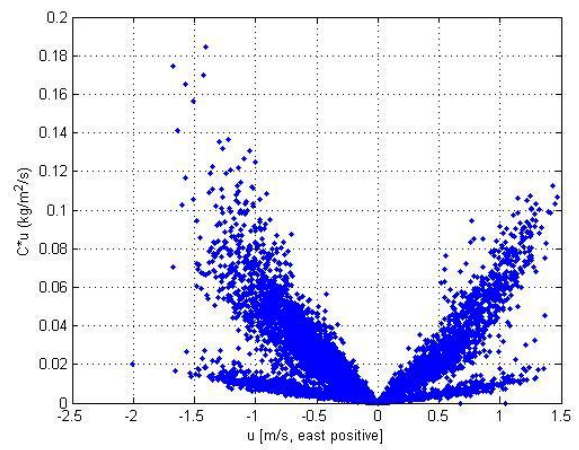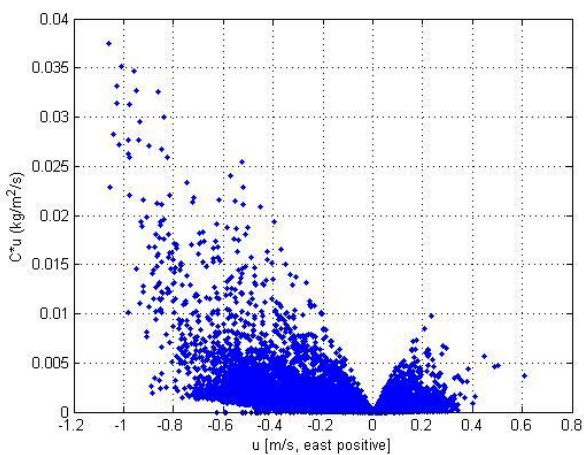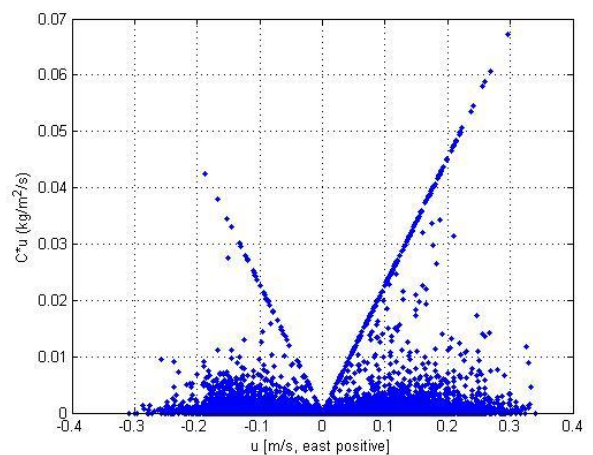
1. Banyan Buoy
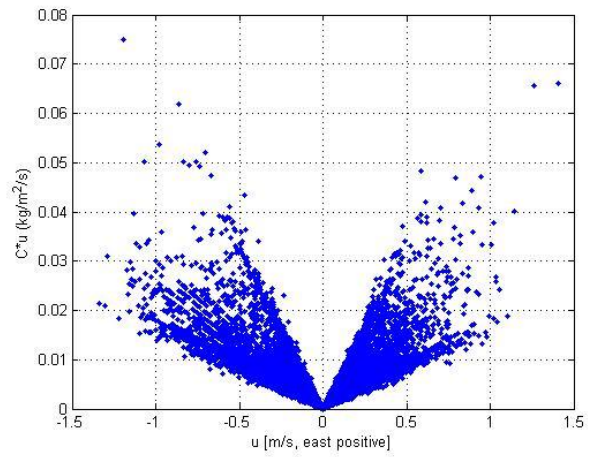
2. Rasubuoy
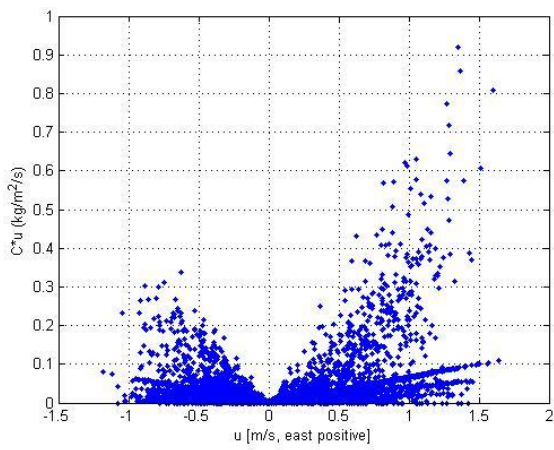
3. Sawabuoy

4. Sisterbuoy

5. Westtuas

6. W2J

Figure 5-2. Sediment flux at all observation points

5.1.3   Spring neap cycle

In this section, variation of sediment concentration and current velocity during fortnightly spring neap cycle will be discussed. Spring neap cycles control sedimentation and suspension of fine sediment, in which large scale erosion and re-suspension occurs during spring tides, increasing the residence time of fine sediment and providing a mechanism for enhancing suspension.

As explained in the Chapter 4, representative data from selected time period will be used to analyze fine sediment during spring neap cycle for both the SW and NE monsoons. During the SW monsoon, representative data is May-June for all observation points, except for Banyan Buoy, whereas during the NE, selected time period is November-December. The fine sediment transport is related mainly to the variation of current velocity rather that to the variation of water level, since variation of water level is relatively the same. Moreover, the flood flow is defined by positive current velocity, where as ebb flow is defined by negative current velocity. The term of spring refers to high water level occurs and neap tide refers to low water level occurs.   Analyses of spring neap time series is described as follows.

5.1.3.1   South-West Monsoon (May-September)

1.   Banyan buoy

Sediment concentration varies during the spring neap cycle, in which high concentration of suspended sediment occurs during spring tide and continues during neap tides (Fig. 5-3). The water level shows semidiurnal signal while current velocities is diurnal. Residual flow is relatively low, which range between 0.1 to 0.2 m/s. During neap tide (09/09/03), current velocities are still stronger and when spring tide (16/09) is progressing current velocities are decreasing. Consequently, sediment concentration is still high during the neap tides because there is enough energy for mixing the fine sediment.

Based on the SSC variation during 24 hours measurement as shown in the Fig.5-4, we can determine the dominant direction of the residual sediment transport, whether it is eastward or westward. It shows that SSC ranges from 10 mg/l to 50 mg/ l and current velocity 1 to 1.5 m/s during spring tide, whereas, SSC ranges 40 mg/l to 60 mg/l at neap tide. During neap tide, flood duration is approximately 11 hours and the rest time is ebb duration. The flood current is higher than the ebb current. Therefore, during neap tide residual flow is more prevail than tidal asymmetry. During spring tide, the flood-ebb duration and current velocities are relatively similar, which imply no residual flow and tide symmetry occurs.

Comparing the hysteresis curves during spring and neap tide, fine sediment is suspended when current velocities are high in both neap and spring tide. Sediment particles settled slightly when current velocity is decreasing during spring tide, and then it is resuspended as current velocity increasing slightly during neap tide. During spring and neap tides, maximum flow velocity dominated by eastward direction.
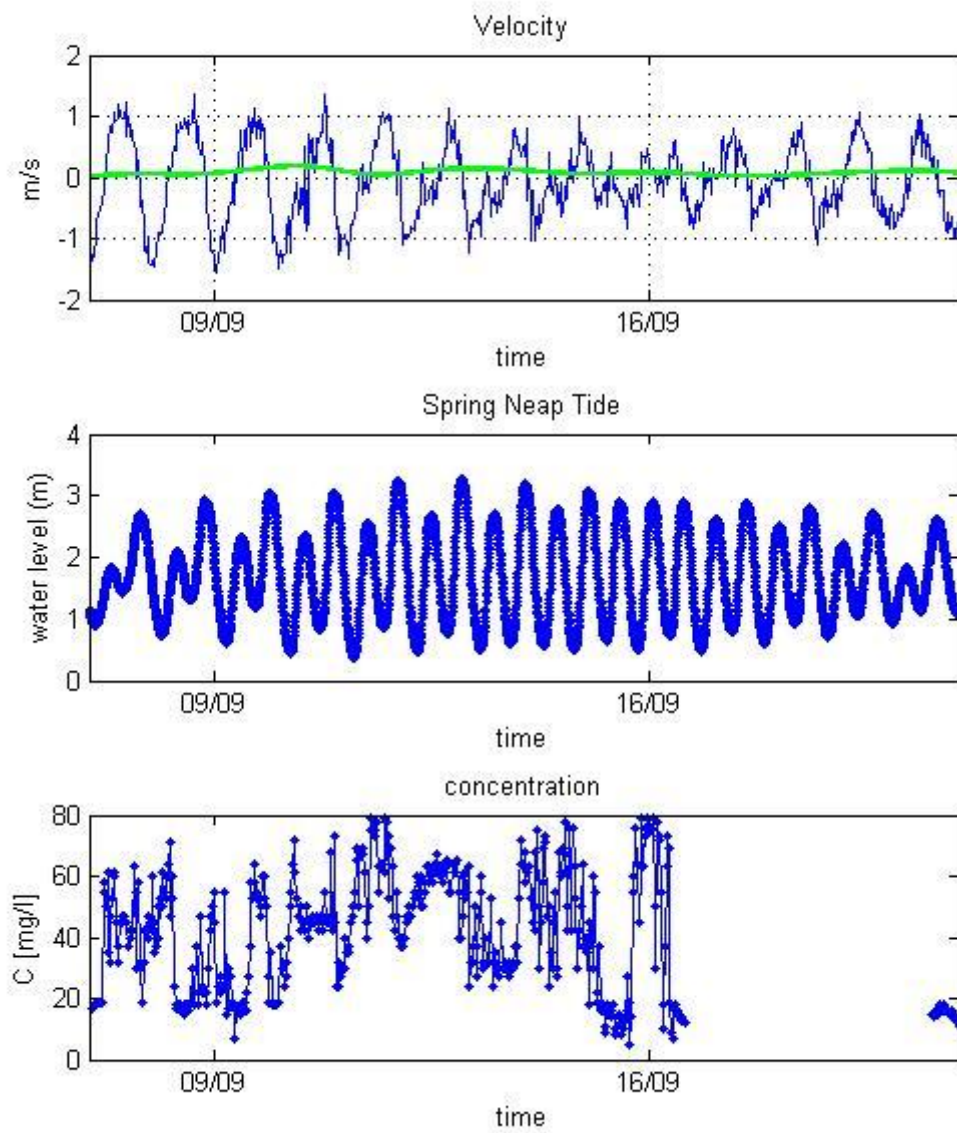
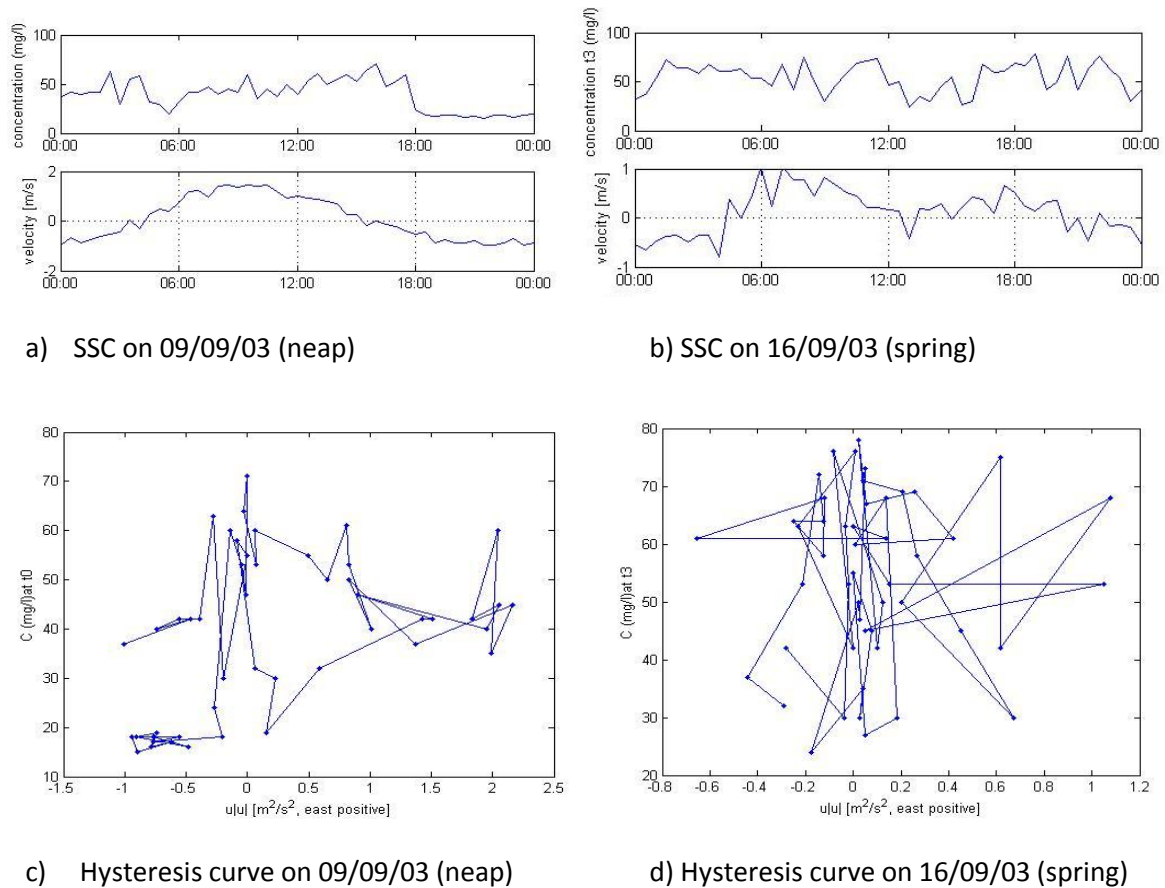Figure 5-3. Spring neap cycle and sediment concentration at Banyanbuoy.

a) SSC on 09/09/03 (neap) b) SSC on 16/09/03 (spring)

c) Hysteresis curve on 09/09/03 (neap) d) Hysteresis curve on 16/09/03 (spring)

Figure 5-4. 24 hours measurement SSC and current velocity at Banyanbuoy

2. Rasubuoy

From Fig 5-5, it can be seen that low current velocity occurs at the beginning of spring tides, and it increases as spring tide is progressing. Sediment concentration range from 20 mg/l to 50 mg/l, and fluctuate as the current velocity rise and fall. SSC at Rasubuoy is higher during neap tide and half spring tide. Compare to the situation at Banyanbuoy, the maximum current velocity at Rasubuoy is lower than that at Banyanbuoy, however, it still strong enough to keep fine sediment in suspension. The 24 hours plotting in the Fig. 5-6 shows that duration of flood and ebb during neap and spring tide are relatively the same. However, during neap tide, the flood current velocity is lower than the ebb current velocity, which results in the residual flow of 0.1 m/s. The flood and ebb current velocities during spring are relatively the same. Moreover, it can be seen that SSC decrease because settling process occurs during slack time of spring tide.

Hysteresis curves show significant differences of residual transport direction during neap and spring tide. There are more SSC are transported towards west during neap tide and relatively symmetrical trend during spring tide. Settling process occurs mainly during half spring, while more SSC become suspension during neap tide. Consider the residual flow

during neap higher than spring, it probably provides enough current to stir the suspended sediment. Therefore, for this specific time period, the role of residual flow relative dominant during the neap tide compare to tidal asymmetry.
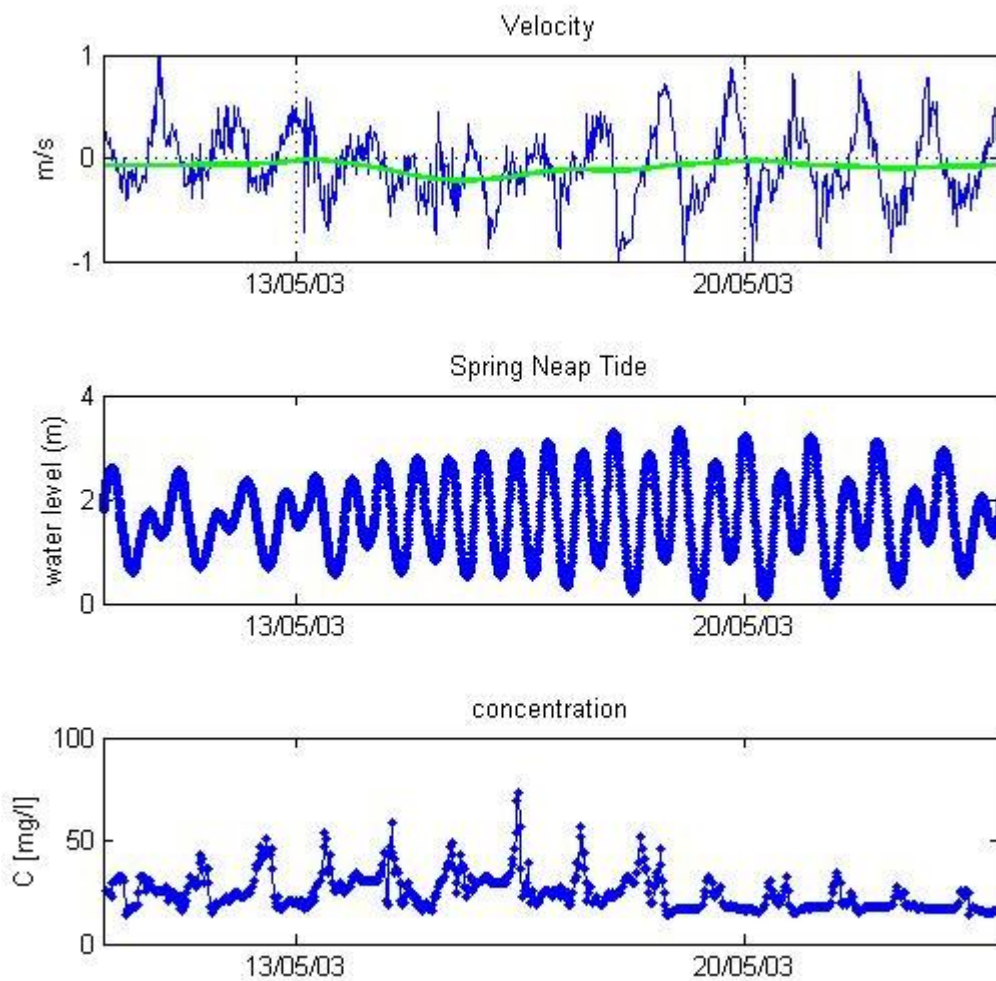

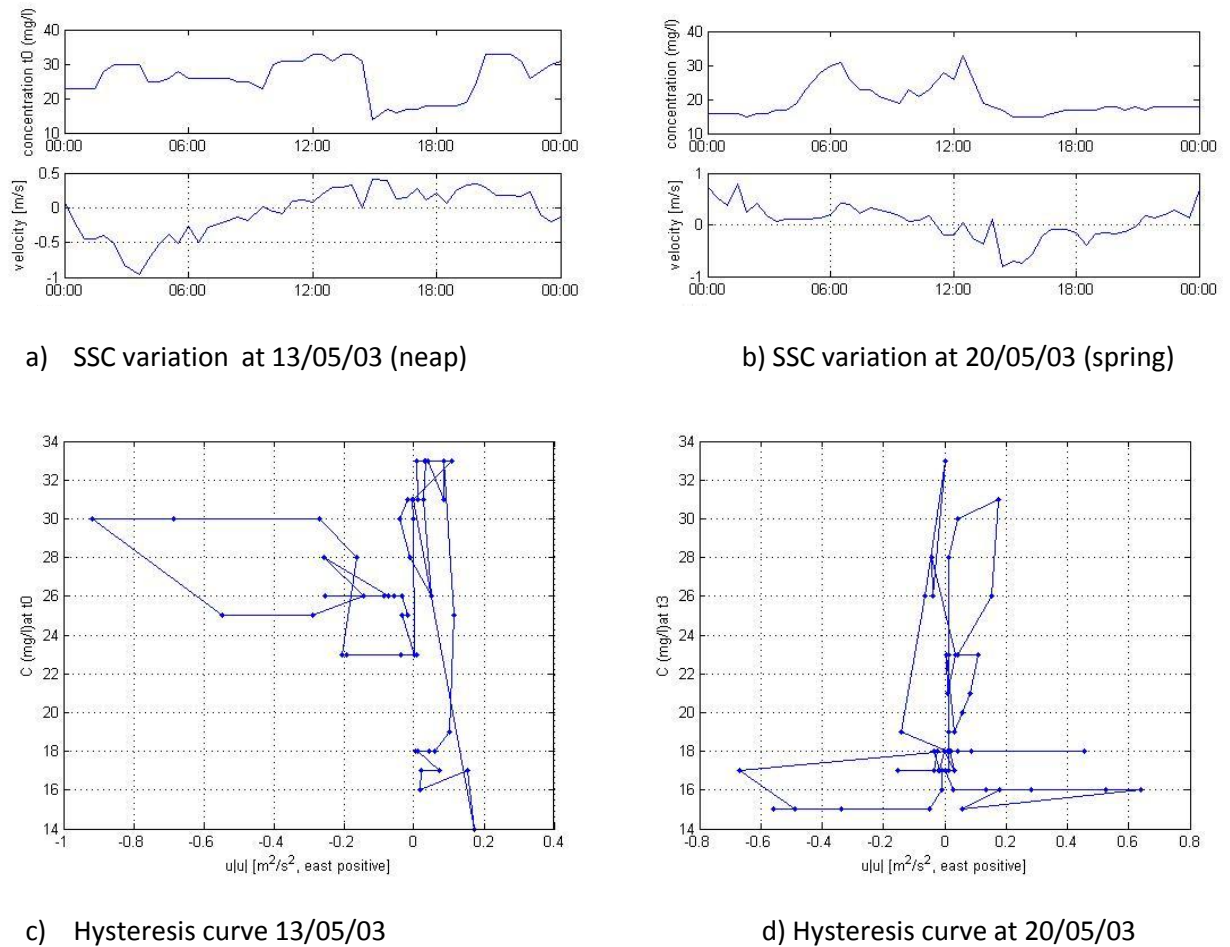Figure 5-5. Spring neap cycle of sediment concentration at Rasubuoy

a) SSC variation at 13/05/03 (neap)

b) SSC variation at 20/05/03 (spring)

c) Hysteresis curve 13/05/03

d) Hysteresis curve at 20/05/03

Figure 5-6. 24 hours measurement SSC and current velocity at Rasubuoy

3. Sawabuoy

Sediment concentration and current velocities at Sawabuoy is shown in the Fig.5-7. Sediment concentration at Sawabuoy is higher than other buoys, which account for more than 500 mg/l, while the current velocity during the spring and neap tide ranges 0.7 to 1.0 m/s. The residual flow velocities ranges from 0.1 to 0.2 m/s. Sediment concentration fluctuates along with changes in current velocity with the highest SSC occurs during half second spring tide.

From 24 hours measurement in Fig 5-8, it shows relative correlation between settling and resuspension processes with the change in current velocities. Sediment concentration in both neap and spring tide are considerably high, but it is observed that during spring tide, SSC is around 100 mg/l to 300 mg/l while SSC range from 200 mg/l to 400 mg/l in neap tide. On the one hand, duration of flood is shorter (approx 8 hours) than ebb (approx 16 hours), for both spring and neap tides. On the other hand, flood current is higher than ebb during spring tide, while in during neap, both currents are relatively the same. Therefore, during

spring tide, the influence of residual flow and tidal asymmetry combined, whereas during neap tide, the residual flow is more dominant.

Hysteresis curve feature residual transport during neap and spring tide. Most of residual transport flow eastward during spring and relatively westward during neap. SSC tend to be in suspension.
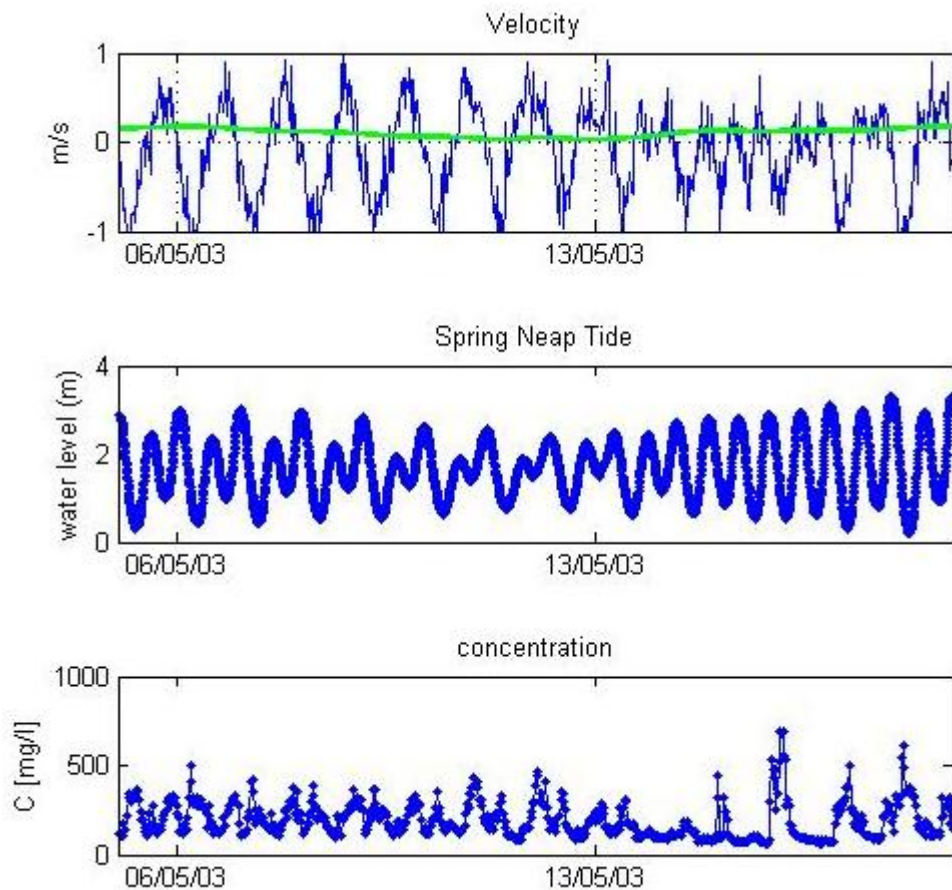

Figure 5-7. Sediment concentration and spring neap current velocity at Sawabuoy
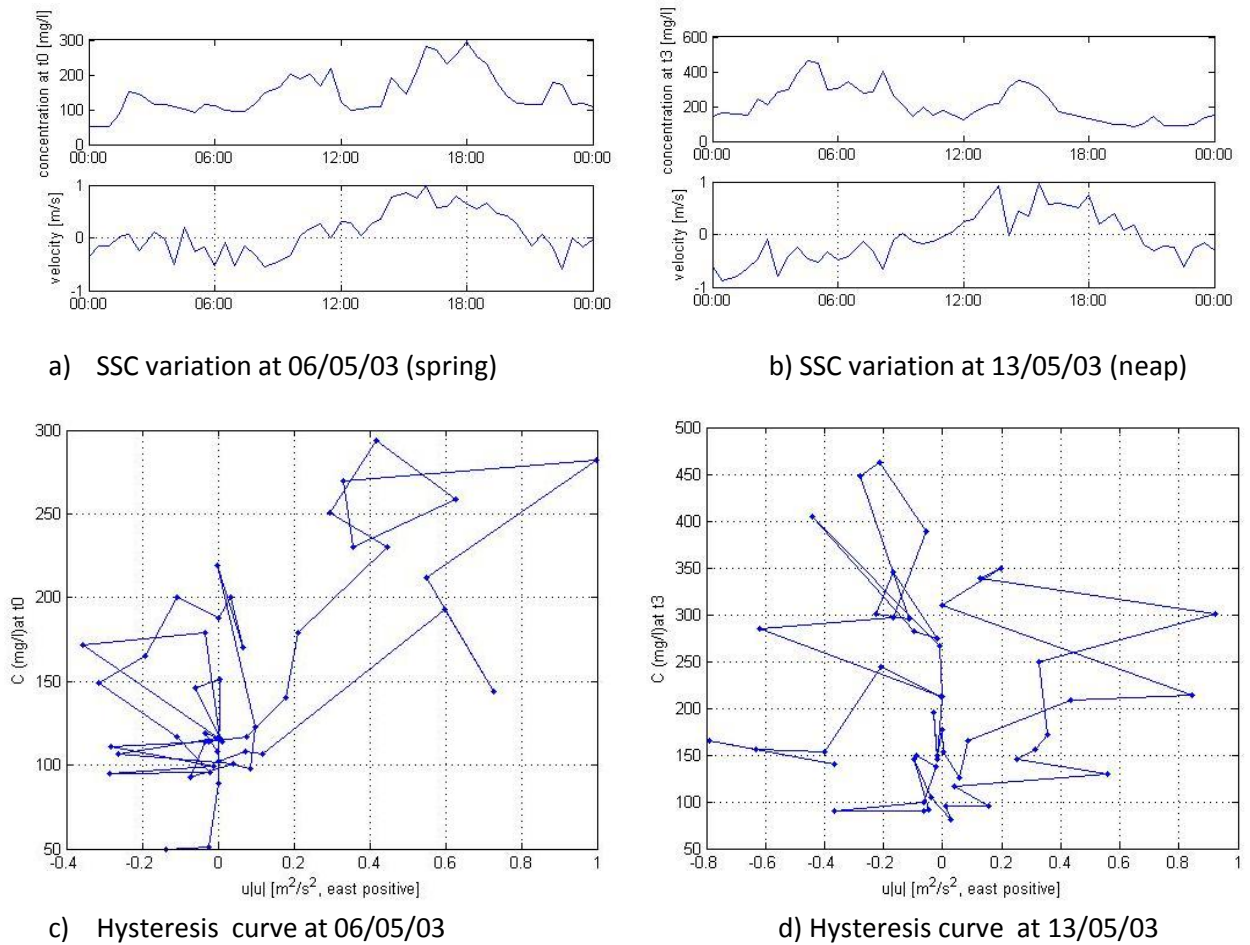
a) SSC variation at 06/05/03 (spring) b) SSC variation at 13/05/03 (neap)

c) Hysteresis curve at 06/05/03 d) Hysteresis curve at 13/05/03

Figure 5-8. 24 hours measurement SSC and current velocity at Sawabuoy

4. Sisterbuoy

As can be seen from Figure 5-9, sediment concentration changes response to the spring neap cycle, in which during spring tide, current velocity is approximately 1 m/s, while during neap tide the current velocity is 0.5 m/s. Residual flow range between 0.1 and 0.2 m/s. Sediment concentration decreasing slightly during neap tide to the range of 40 mg/l to 50 mg/l and increasing during spring tide to almost 80 mg/l.

From 24 hours measurement as shown in the Figure 5-10, it is observed that settling process occurs during slack time in both spring and neap tide and resuspension occurs as current velocity increases. Flood duration during spring is shorter than ebb duration (8 hours compare to 16 hours), while during neap, the duration of flood and ebb are both relatively similar (6 hours). The current velocity of flood and ebb are relatively the same (1 m/s) for both spring and neap tide. Hence, during spring tide, residual flow and tidal asymmetry affect the residual transport, while during neap tide; only residual flow is counted to affect residual transport. Moreover, residual transport direction from hysteresis curves show a

dominant westward flow during spring, whereas, eastward direction dominates during neap.
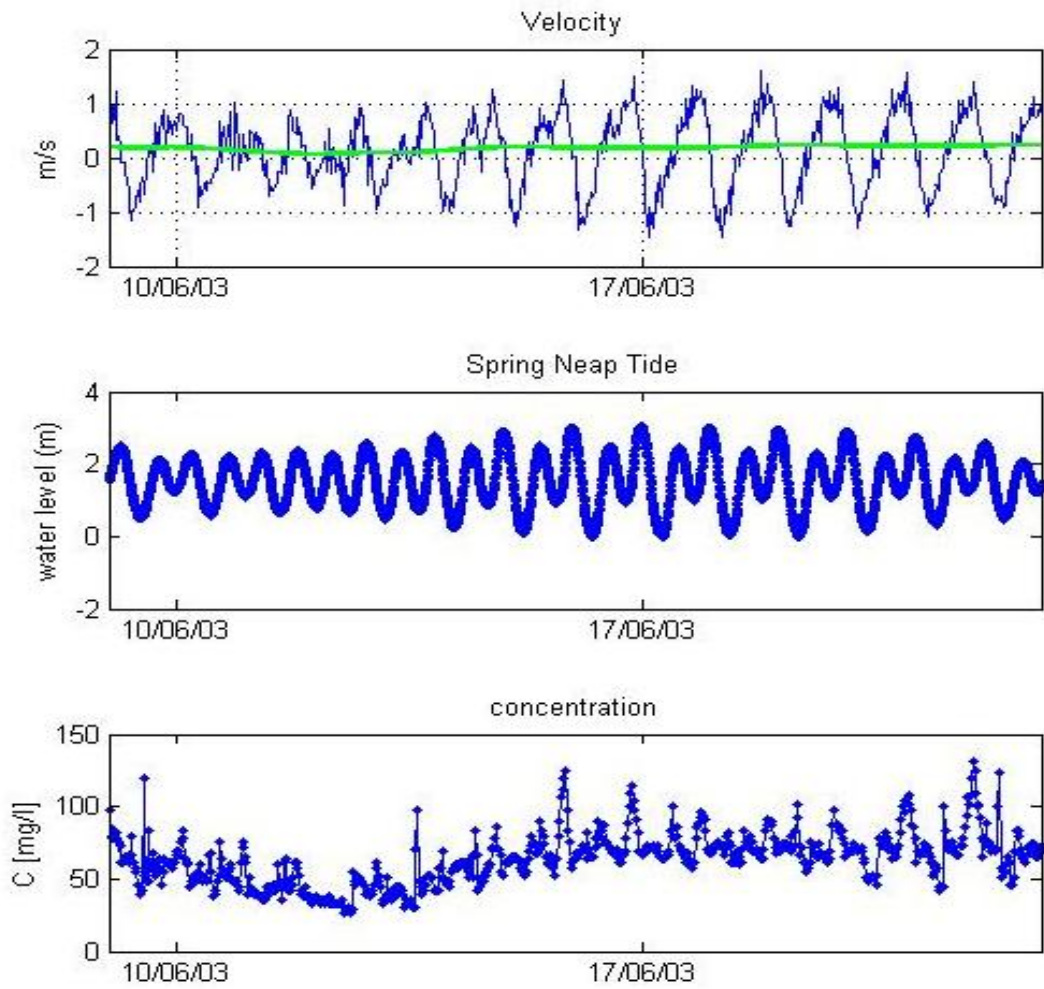

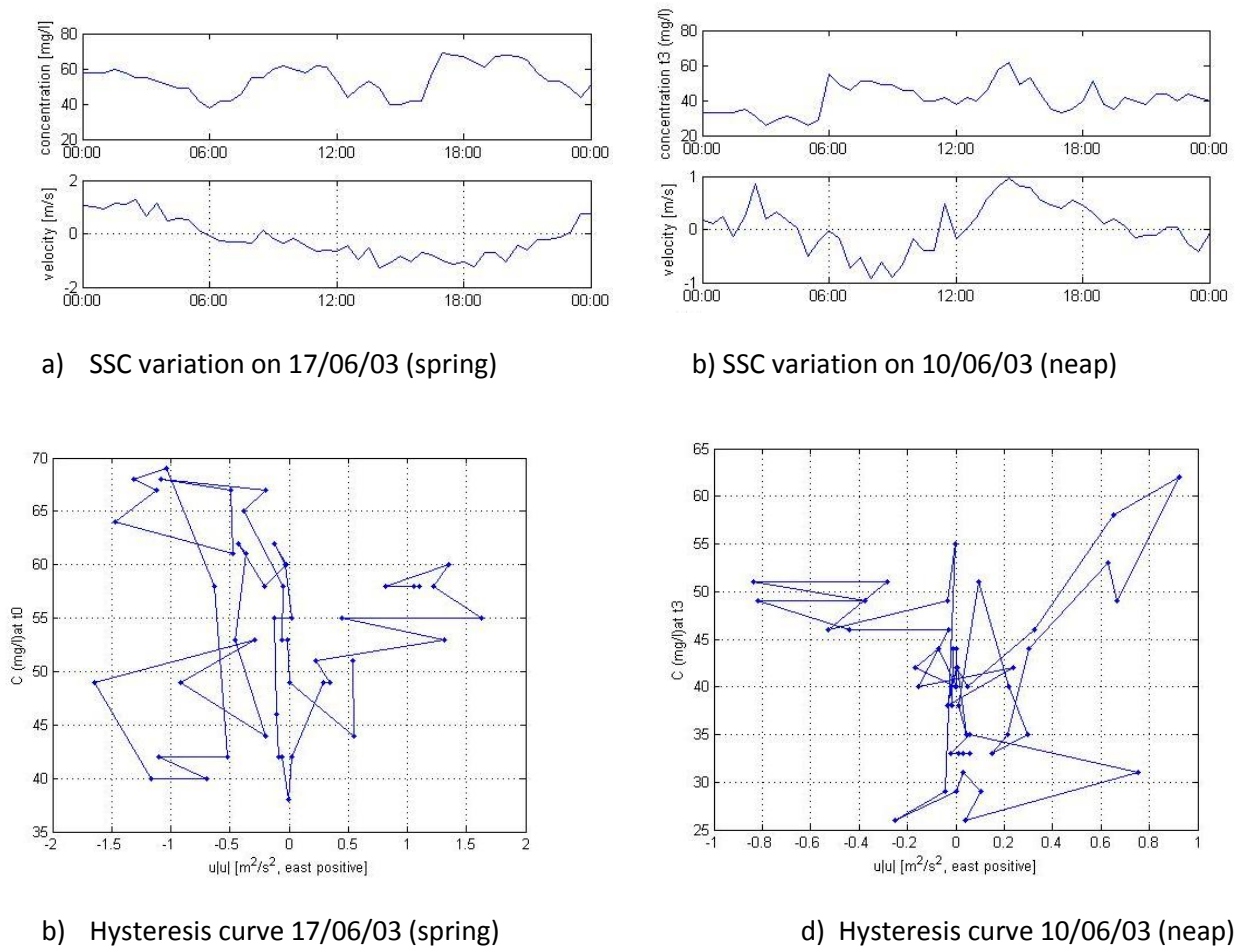Figure 5-9. Sediment concentration and current velocity at Sisterbuoy

a) SSC variation on 17/06/03 (spring)   b) SSC variation on 10/06/03 (neap)

b) Hysteresis curve 17/06/03 (spring)   d) Hysteresis curve 10/06/03 (neap)

Figure 5-10. 24 hours measurement SSC and current velocity at Sisterbuoy

5. Westtuas

The sediment variation during spring neap cycle is shown in the Fig 5-11 and Fig. 5-12. Sediment concentration during this time period mostly is below 20 mg/l, although there are some rising SSC to almost 60 mg/l during transition of neap to spring. The current velocity ranges between 0.5 m/s during spring tide and 0.2 m/s during neap tide. Both tidal elevation and the current velocity show relatively semidiurnal signal. In general, current velocities during spring tide are higher and neap tide, which ranges from 0.2 during neap and 0.5 during spring. Residual flow ranges between 0.1 to 0.2 m/s. Picking up and suspension process mainly occurs during the transition of neap to spring which indicated by higher SSC. From the 24 hours measurement in Fig 5-12, flood and ebb duration for spring tide are relatively the same, while during neap, it is not really clear. However, considering the current fluctuation, the ebb duration is longer than flood duration. This implies, during spring tide, tidal is relatively symmetric and residual flow is dominant to cause sediment transport. The residual transport dominantly flows westward for both spring and neap tides.
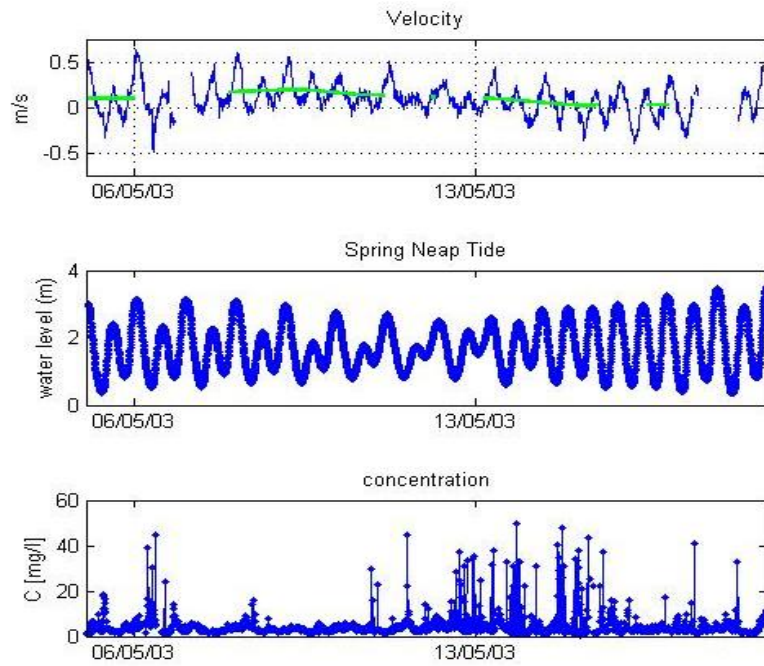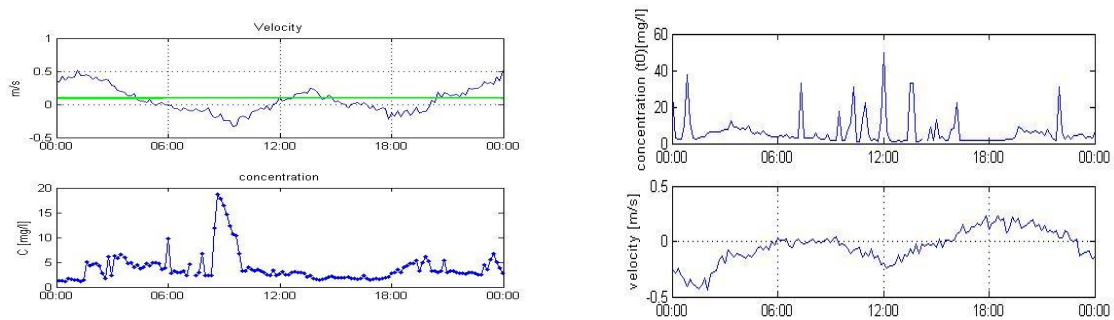
Figure 5-11. Spring neap cycle of sediment concentration and current velocity at Westtuas

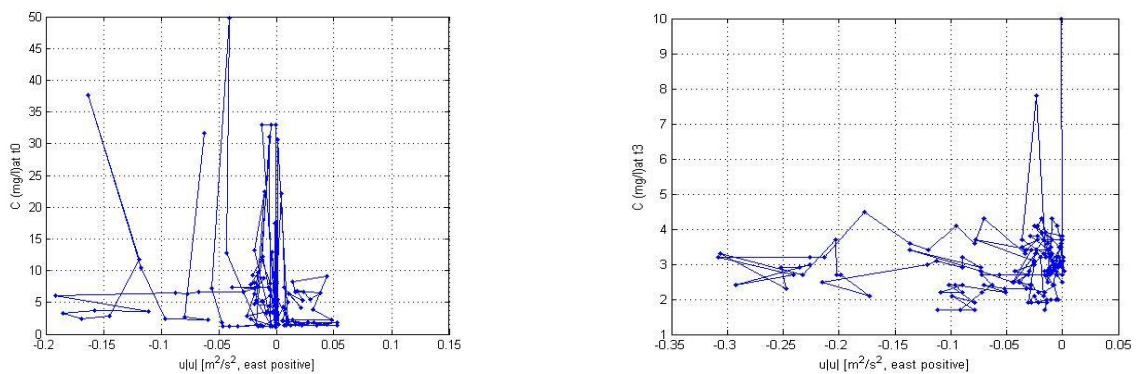a) SSC variation on 06/05/03 (spring) (neap)

b) SSC variation on 13/05/05

Figure 5-12. 24 hours measurement SSC and current velocity at Westtuas

6. W2Jbouy

Sediment concentration variation and current velocity during spring neap cycle is shown in Fig. 5-13 and Fig 5-14. SSC and current velocity are lower during neap than during spring. Current velocities range from 0.2 to 0.4 m/s during spring, and 0.1 to 0.2 m/s during neap tide. Residual flow is relatively small compare to other buoys, which ranges between 0 to 0.05 m/s. Tidal current phase is relatively similar to the tidal elevation phase. Sediment concentration variations are more responsive to current velocity variations during spring tide than neap (Fig 5-14). The 24 hours measurement in Fig 5-14 indicates duration of flood and ebb are relative the same during spring, while flood duration is longer during neap. This implies during spring, tidal asymmetry contribute more in fine sediment transport than residual flow as well as during neap. Moreover, hysteresis curves show dominant maximum flow direction to westward of high SSC during neap and spring tide, whereas it is eastward for low concentration for both spring and neap.
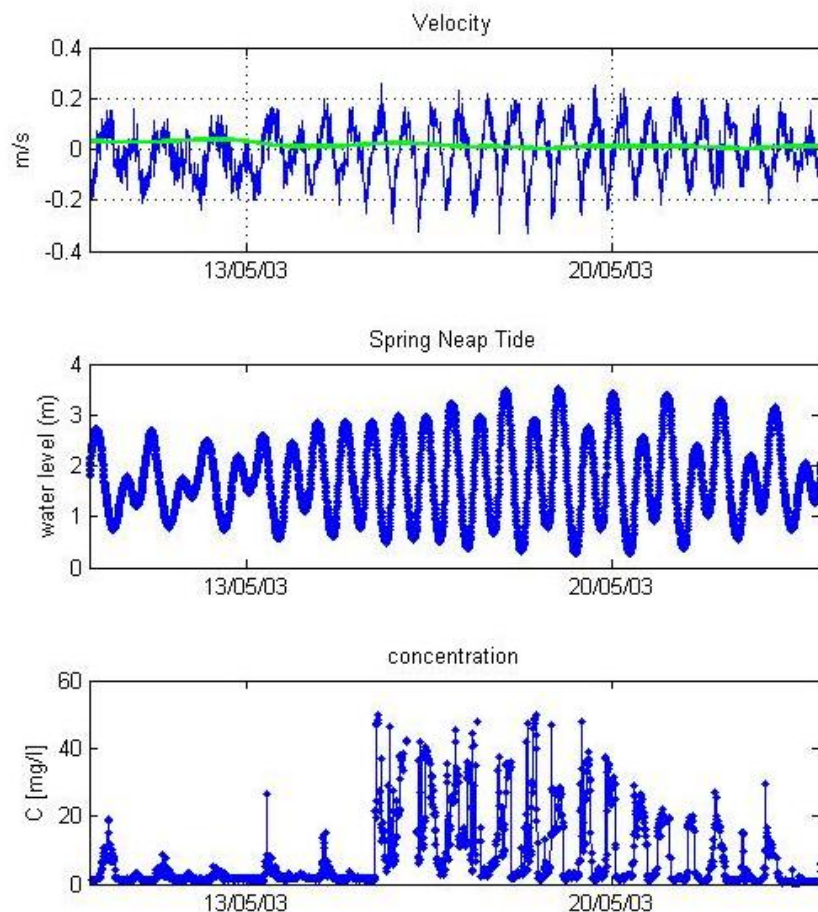

Figure 5-13. Spring neap cycle of sediment concentration and current velocity at W2J buoy

a) SSC variation on 13/05/03 (neap)   b) SSC variation on 20/05/03 (spring)

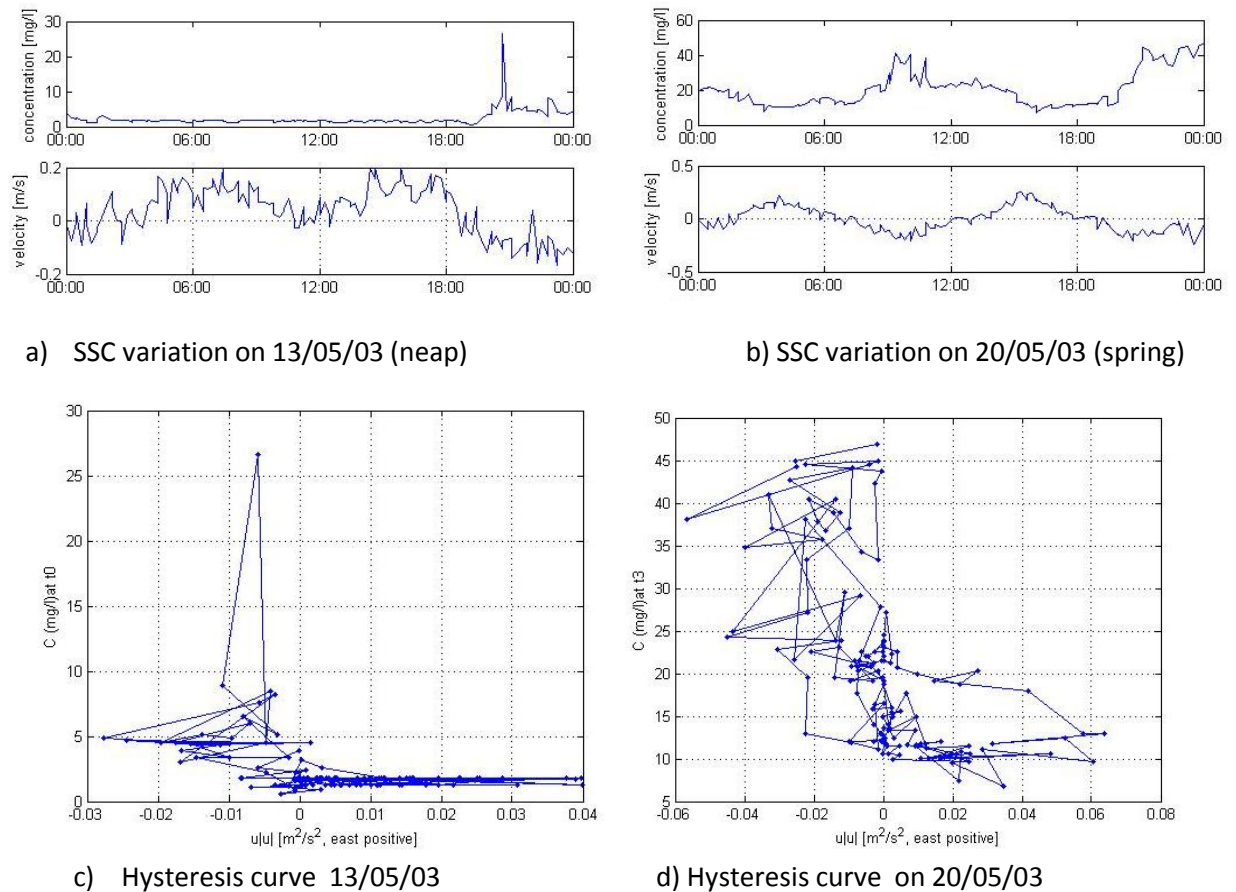c) Hysteresis curve 13/05/03   d) Hysteresis curve on 20/05/03

Figure 5-14. 24 hours measurement SSC and current velocity at W2Jbuoy

Summary of analysis to determine relative influence of residual flow and tidal asymmetry in the fine sediment transport is shown in the Table 7. In general, during the SW monsoons, it can be said that residual flow influences more significantly than tidal asymmetry. Tidal asymmetry plays major influence at W2J which is located in the close to Jurong, where it is expected tidal system is semidiurnal and tide induced hydrodynamic is dominant.

Table 7. Summary of spring neap analysis during SW monsoon

Buoys	Rotation	Current (m/s)		Residual transport		Concentration range (mg/l)		Tidal and current signal	Relative driven mechanism	
		Spring	Neap	Spring	Neap	Spring	neap		Spring	Neap
Banyan	-50	1.5	0.5	eastward	eastward	20-60	50-80	Mixed	Residual flow	Residual flow
Rasu	-75	1	0.5	westward	symmetric	10-40	30-40	Mixed	Residual flow	Residual flow
Sawa	-60	1	1	eastward	eastward	400	400	Mixed	Combined of tidal asymmetry and residual flow	Residual flow
Sister	60	0.5	0.7	westward	westward	40-80	20-40	Mixed	Combined of tidal asymmetry and residual flow	Residual flow
West Tuas	1	0.5	0.2	westward	westward	10-15	5-10	Semidiurnal	Residual flow	Not clear
W2J	-50	0.2	0.2	westward	westward	20-40	10-20	Semidiurnal	Tidal asymmetry	Tidal asymmetry

5.1.3.2 North-East Monsoon (November-March)

1. Banyanbuoy

Data from Banyanbuoy is limited and there a lot of gap, in particular during NE monsoon moths. Therefore, the representative data for this time period is not available.

2. Rasubuoy

Sediment concentration variation and current velocities are shown in the Fig 5-15 and Fig 5-16. The level of sediment concentration during the NE monsoon is higher compared to the sediment concentration during the SW monsoon. SSC mostly ranges between 60 mg/l to 70 mg/l, while the current velocity is relatively lower during neap (0.5 mg/l) and higher during spring (1 m/s). Residual flow ranges between 0 to 0.2 m/s. From 24 hour plotting (Fig. 5-16,) it also can be seen that SSC are relatively constant and slightly increase at beginning of spring tide. Moreover, flood duration and ebb duration during spring are relatively the same, although it is not showing clearly. Similar to the spring tide, it is difficult to distinguish duration of flood and ebb because of irregularity of data. However, it can be expected that residual flow mainly influence the sediment transport during both spring and neap tide. Hysteresis curves shows significant difference that during neap tide, maximum flow direction is relative symmetric, while during spring it is dominated by westward flow.
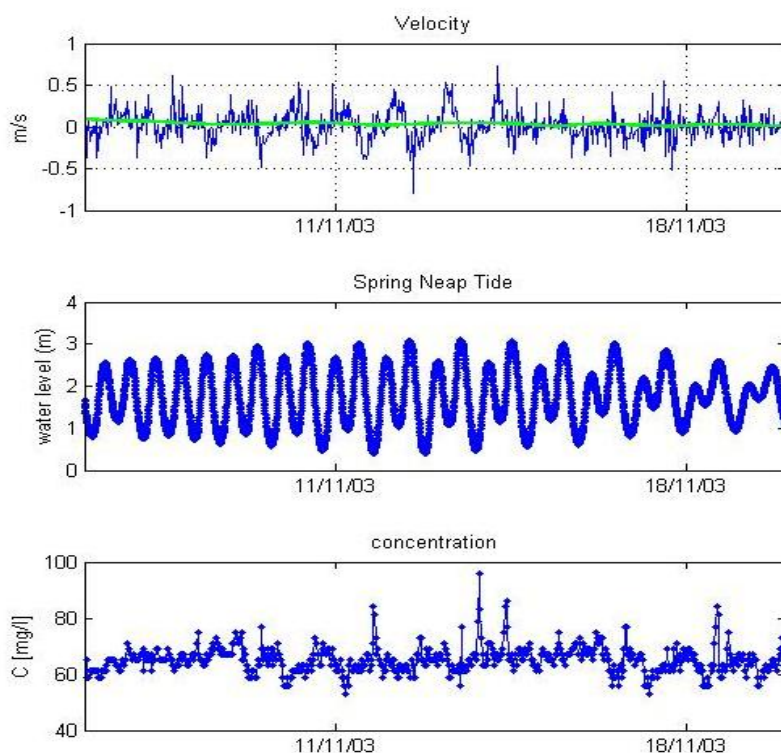

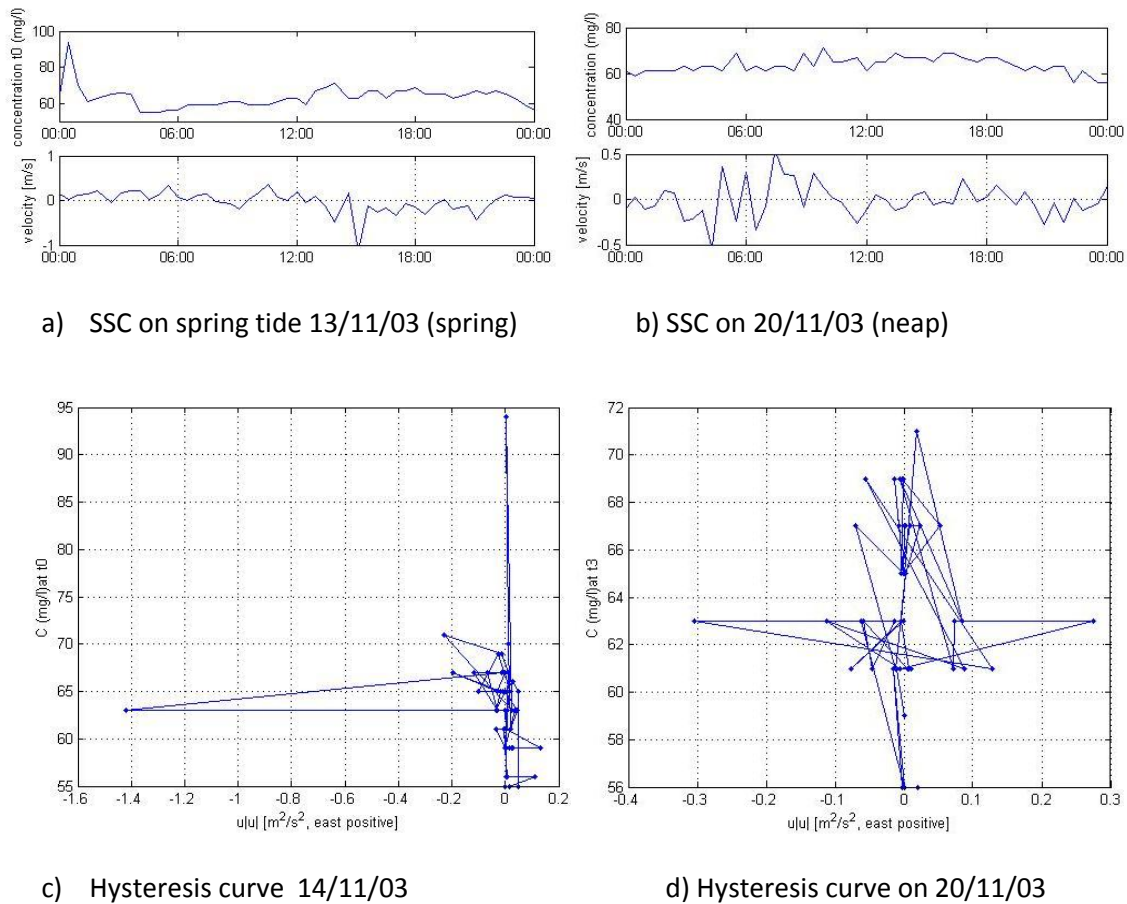Figure 5-15. Sediment concentration and current velocity at Rasubuoy, NE monsoon

a) SSC on spring tide 13/11/03 (spring)   b) SSC on 20/11/03 (neap)

c) Hysteresis curve 14/11/03   d) Hysteresis curve on 20/11/03

Figure 5-16. 24 hours measurement SSC and current velocity at Rasubuoy, NE monsoon

3. Sawabuoy

Sediment concentration at Sawabuoy is lower than concentration during summer monsoon and it ranges between 20 mg/l to 50 mg/l (Fig 5-17). Tidal current velocity is lower than tidal current during summer monsoon; however the residual flow is relatively the same, which ranges from 0.1 to 0.2 m/s. SSC become more suspended during the end of spring until neap tides, whereas some of sediment settled during spring. This is probably caused by relatively large fine sediment with high fall velocity than the current velocity. Moreover, from 24 hours measurement, it is noted that flood duration is shorter than ebb duration during neap tide, while during spring tide flood and ebb durations are relatively symmetrical. The flood velocity during spring is higher than ebb current. Therefore, in term or relative contribution of tidal asymmetry and residual flow to fine sediment transport, it can be said that during neap tide, tidal asymmetry combined with residual flow to influence fine sediment transport, while during spring, residual flow contribute more that tidal asymmetry. Moreover, hysteresis curves show more residual transport towards west during neap and spring.
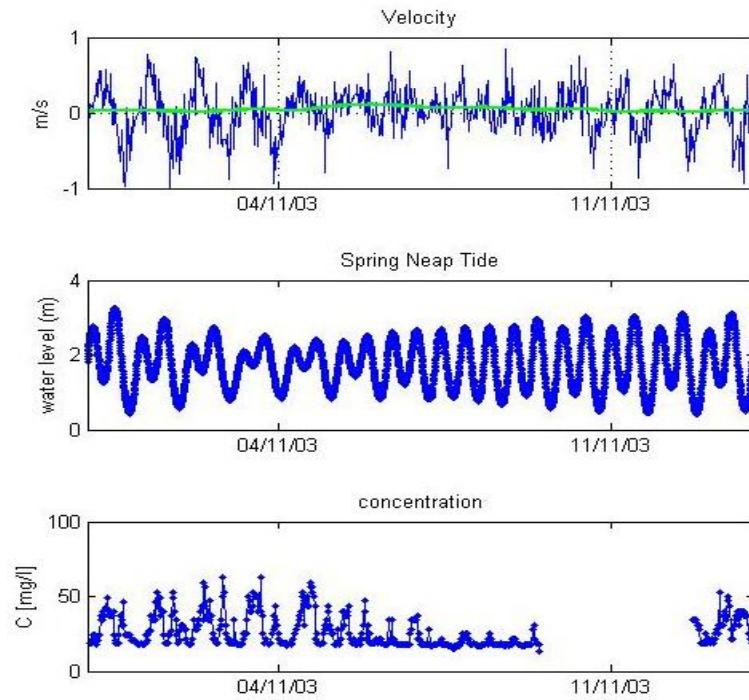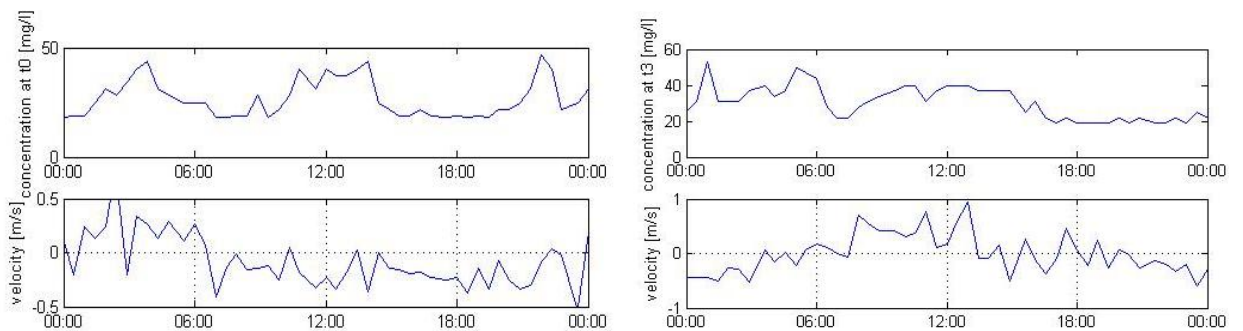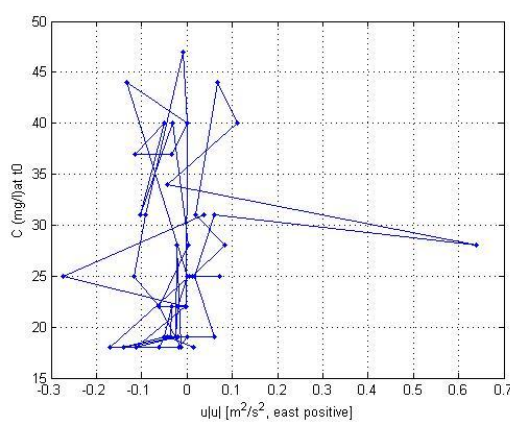
Figure 5-17. Sediment concentration and current velocity at Sawabuoy, NE monsoon
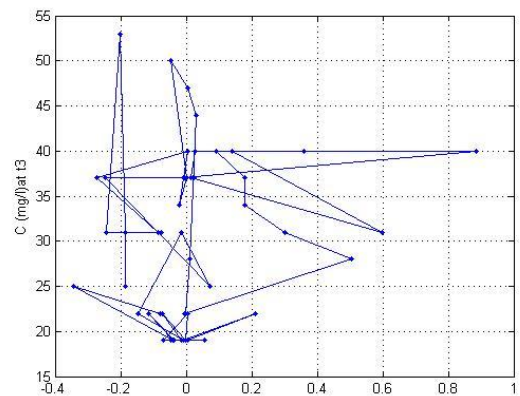

a) SSC variation on 04/11/03 (neap)

b) SSC variation on 14/11/03 (spring)

c) Hysteresis on 04/11/03

d) Hysteresis on 14/11/03

Figure 5-18. 24 hours measurement SSC and current velocity at Sawabuoy, NE

4. Sisterbuoy

Sediment concentration variation and current variation is shown in Fig 5-19 and Fig 5-20. Compared to SSC during the SW monsoon, SSC observed during this specific time periods in the NE monsoon season is far lower. It ranges between 10 mg/l to 20 mg/l. The cause of this extreme difference is not clear due to limited information of historical high load discharge from sediment sources. Current velocities are relatively the same as current during summer monsoon although the residual current is clearly higher than it is during summer monsoon (ranges from 0.2 to 0.5 m/s).

From Fig 5-20, it can be seen that flood and ebb duration during both spring and neap tide are relatively the same. However, the length of flood-ebb duration during spring is longer than during neap tide (approx. 10 hours compared to approx. 6 hours). This implies relative influences of residual flow than tidal asymmetry fine sediment transport during spring. Moreover, hysteresis curves show dominant westward flows for both neap and spring tides
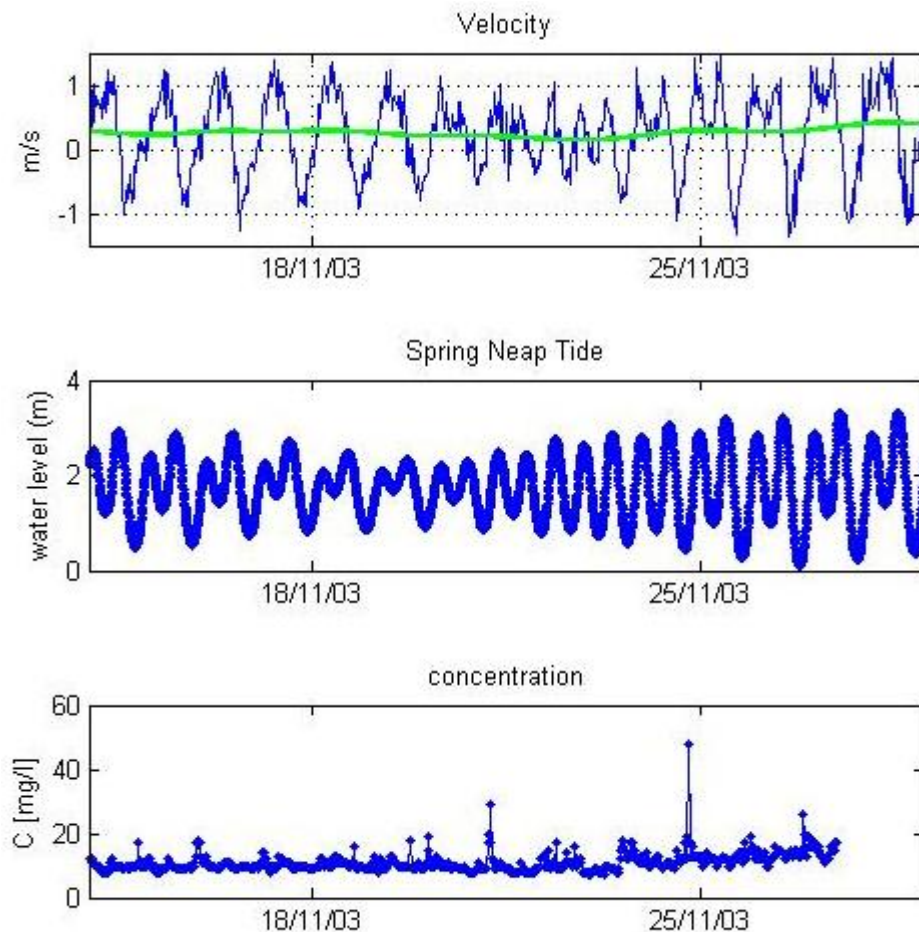

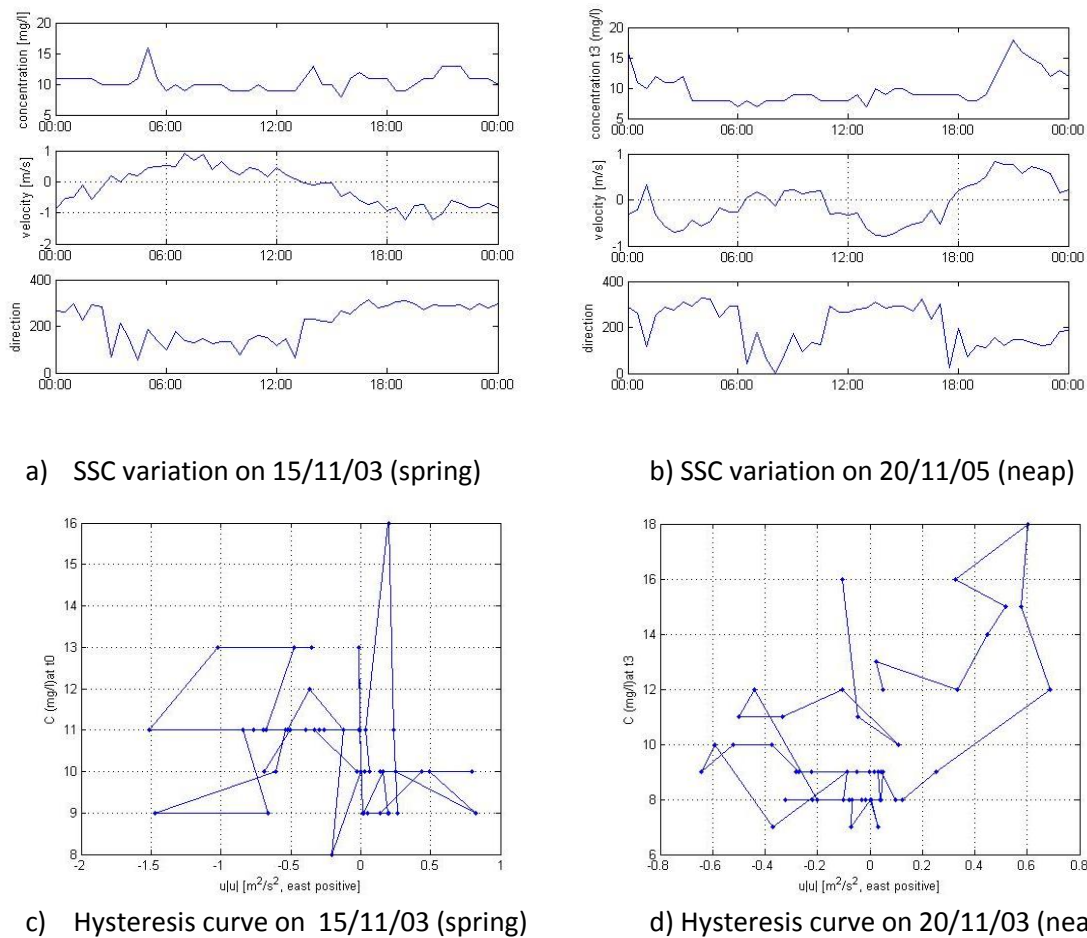Figure 5-19.Sediment concentration and current velocity at Sisterbuoy, NE monsoon

a)   SSC variation on 15/11/03 (spring)   b) SSC variation on 20/11/05 (neap)

c)   Hysteresis curve on 15/11/03 (spring)   d) Hysteresis curve on 20/11/03 (neap)

Figure 5-20. 24 hours measurement SSC and current velocity at Sisterbuoy, NE monsoon

5. Westtuas

Data on current velocity from Westtuas is limited and there are several missing time serried. Moreover, the available data often is discontinuing that it is impossible to take complete spring neap time period. Therefore, the analysis of fine sediment transport during the NE monsoon cannot be delivered.

6. W2J

Sediment concentration variation and current variation is shown in Fig 5-21 and Fig 5-22. Sediment concentration measured at this buoy is relatively low in which mostly the concentration is below 10 mg/l. The current velocity is higher during spring than neap. From Fig 5-22, it can be seen that flood-ebb current velocity duration for during both spring and neap are relatively symmetrical. Therefore, residual flow influences more to fine sediment transport than tidal asymmetry. In addition, hysteresis curves show relatively westward dominant residual transport during both neap and spring tides.
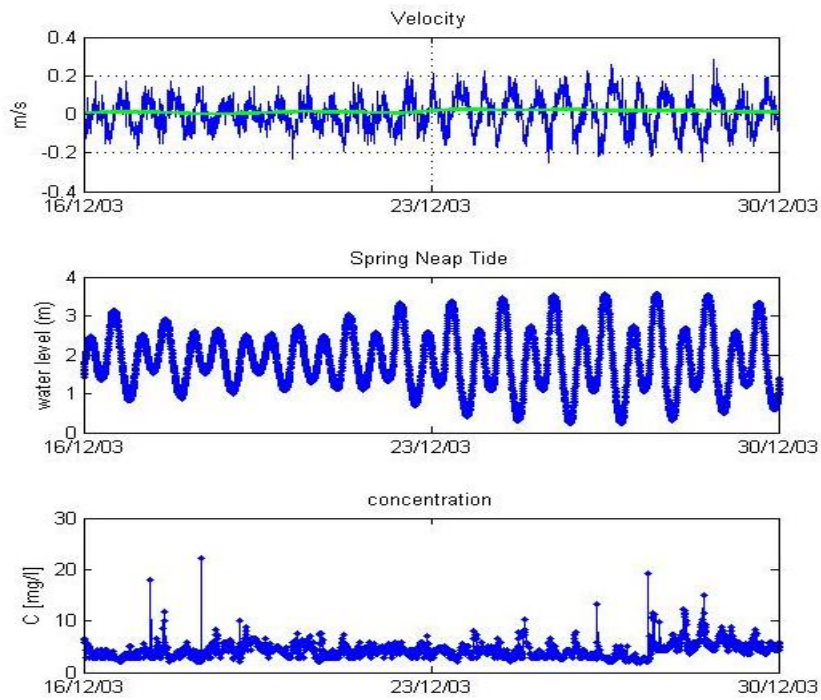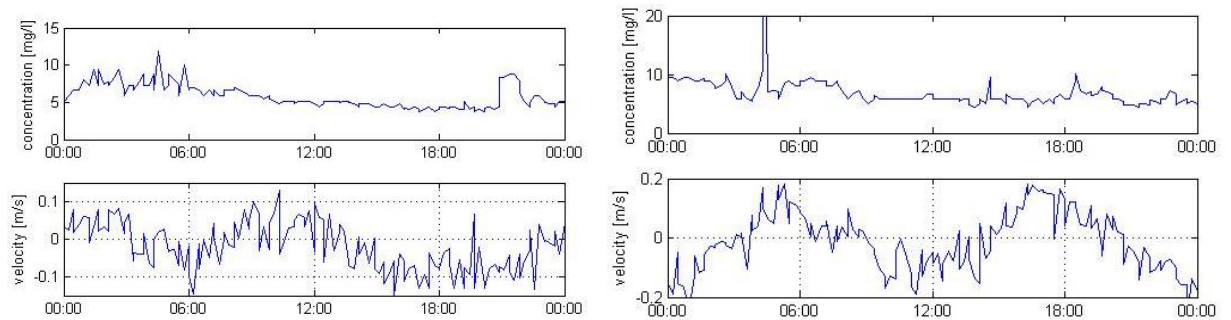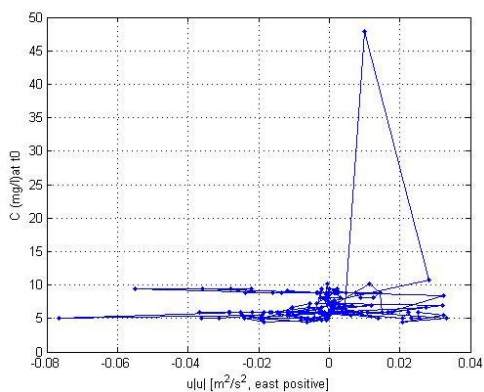
Figure 5-21. Sediment concentration and current velocity at W2J buoy
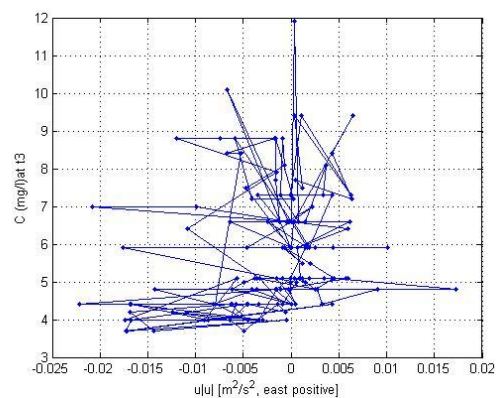

a)   SSC variation on 17/12/03 (neap)   b) SSC variation on 20/12/03 (spring)

c). Hysteresis on 17/12/03   d) Hysteresis on 20/12/03

Figure 5-22. 24 hours measurement SSC and current velocity at W2J, NE monsoon

Summary of analysis to determine relative influence of residual flow and tidal asymmetry in the fine sediment transport during the NE monsoon is shown in the Table 8. In general, residual flow play significant influences to fine sediment transport compared to tidal asymmetry. This is similar to driven mechanism of fine sediment transport during the SW monsoon. Moreover, transport direction during spring and neap is dominated by westward direction except at Rasubuoy, where transport direction during neap is mixed direction. Sediment concentration generally is lower compared to sediment concentration during the SW monsoons.

Table 8. Summary of spring neap analysis during NE monsoon

Buoys	Rotation	Current (m/s)		Residual transport		Concentration range (mg/l)		Tidal and current signal	Relative driven mechanism	
		Spring	Neap	Spring	Neap	Spring	Neap		Spring	Neap
Banyan	-50	Not available								
Rasu	-75	0.5	0.2	westward	symmetric	10-40	10-20	Mixed	Residual flow	Residual flow
Sawa	-60	1	0.5	westward	westward	20	50	Mixed	Combined of tidal asymmetry and residual flow	Residual flow
Sister	60	1.5	0.7	westward	westward	10-20	10-30	Mixed	Residual flow	Residual flow
West Tuas	1	Not available								
W2J	-50	0.2	0.2	westward	westward	<10	10-20	Semidiurnal	Residual flow	Residual flow

6   Discussion

This chapter discusses results from data analysis on the fine sediment transport near fringing coral reefs islands in the Singapore Strait. Fine sediment transport is important to understand the impact of sedimentation and turbidity to the coral reefs. Moreover, it also identifies driven mechanism of fine sediment transport and turbidity, seasonal variation of sediment concentration and current velocity.

6.1   Seasonal variation of fine sediment transport

Seasonal variation of fine sediment transport is determined by analysis the concentration variation during both southwest and northeast monsoon. Physical oceanography and climatology that influence and govern fine sediment transport in the area are illustrated in the Figure 6.1. Respectively, the northeast monsoon coincides with the wet season, which brings more rainfall to the area. Moreover, average residual current velocity during NE range from 0.1 to 0.3 m/s and peak in January, which account for 0.8 m/s. Residual flow direction is dominated by westward direction (Figure 5-1), except during transition periods, the flow direction is slightly random. During this time period, discharge from the Johor River higher and transport more sediment to the strait. Rough estimation of Johor river discharge of suspended sediment load   to the coral reefs islands is about 1.6×10^3 kg/s, which derive from assumptions of average suspended sediment concentration of 1 g/l; average discharge of 37.5 m^3/s; average residual flow of 0.3 m/s, and average distance of 40 km from corals reefs islands. This rough estimation neglect sediment dynamic such as settling process and deposition of sediment. However, the 1.6×10^3 kg/s will significantly affect the sediment load to the coral reefs. Moreover, coupling between tidal current and monsoon driven current, including wind driven through-flow influence the large scale of fine sediment transport in the strait.
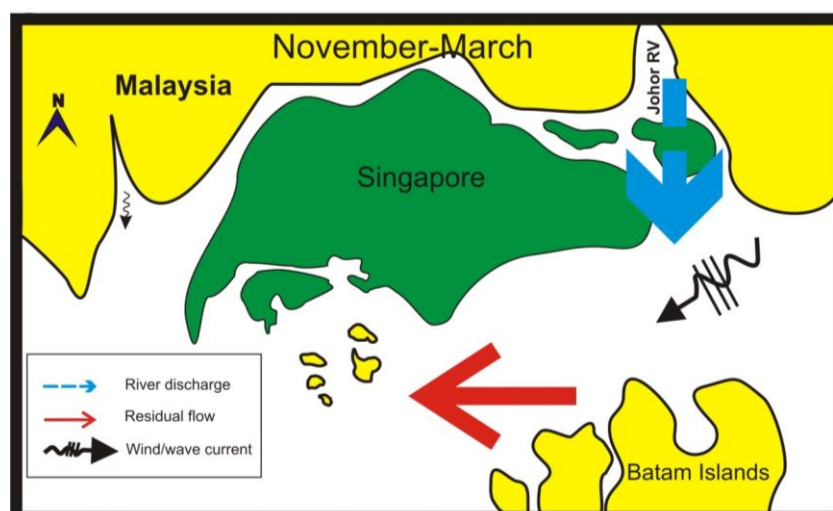

Figure 6-1. General pattern of driven mechanism of sediment transport during NE monsoon

During southwest monsoon, the reserve mechanism occurs. The southwest monsoon coincides with the summer season, in which less rain and discharge flow into the strait. Considering larger areas and stronger wind speed, it is possible longer fetch can develop to cause higher wind generated waves. Residual current ranges from 0.1 to 0.3 m/s whith dominant direction towards east. Moreover, the south equatorial current (SWC) also develops due to hydrodynamic pressure gradient between the South China Sea and the Malacca Strait and the Indian Sea, which lead to general eastward transport flow.
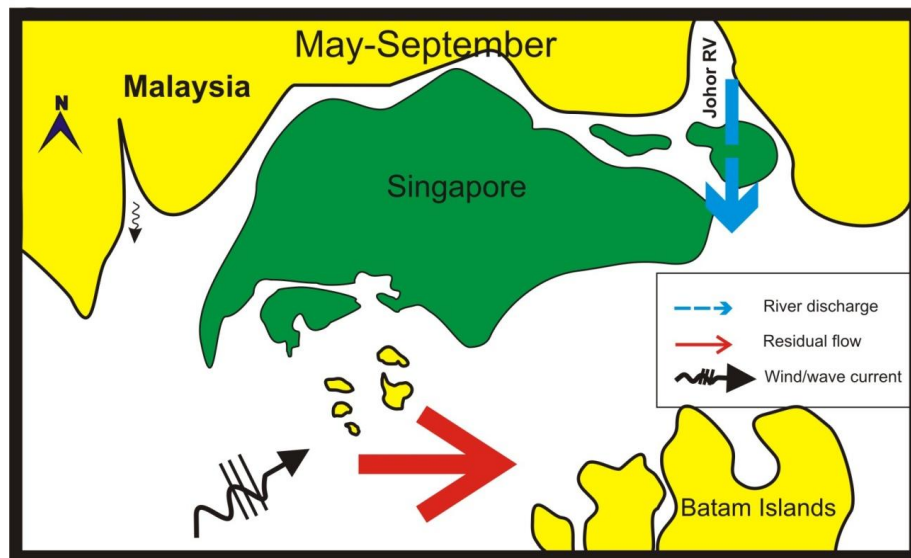

Figure 6-2. General pattern of driven mechanism of sediment transport during SW monsoon

6.2   Tidal and residual flow

Based on field data, an assumption that was made for this study that sediment transport is dominated by suspended load transport since suspended sediment plays major role in increasing of turbidity around coral reefs islands of Singapore. Therefore the maximum velocity is higher than settling velocity of sediment particles.

Analysis on sediment concentration variation during spring neap cycle shows direct response of sediment concentration to tidal cycle and variations in current velocities. Sediment concentration variations were observed during different representative time period in both the SW and NE monsoons. The representative of the SW is May-June for most observation points, except Banyanbuoy, whereas representative time period of the NE monsoon is November and December. The selection of representative time period was based on the availability and the quality of the field data.

In general, residual flow are observed through all time period, which the highest residual flow of 80 cm/s occurs in January 2003 at Banyanbuoy, and the average range is from 0.1 to 0.4 m/s. Residual flow direction is dominated by eastward flow during SW monsoon and by westward flow during NE monsoon (Figure 5-1). Moreover the tidal elevation shows

semidiurnal signal while current velocity shows diurnal signal. Location of Singapore Strait between two major tidal systems results in complex tidal system in the region.

In terms of relation between sediment concentration and current velocity, it is expected that sediment concentration increase or higher when the current velocity is high because there are more sediment particles will be suspended and eroded during high current velocity. However, from the results of spring neap analysis, it is often not the case. At most of the time during selected spring neap cycle, sediment concentrations are in suspension. For example, in Sawabuoy and Sisterbuoy, sediment resuspension occurs during low current velocity (Figure 5-8,Figure 5-9). Moreover, the slight settling process occurs during the slack tide. However, because the duration of slack tides is relatively short both during flood and ebb, it results in small decrease of sediment concentration, as observed almost at all observation points.

Furthermore, sediment concentration during SW generally is higher that concentration during NE monsoon. Significant difference can be observed at Sawabuoy, Sisterbuoy and Rasubuoy, where the concentration difference is really high. However, the cause of such high concentration is still unclear due to limitation of historical data from other sediment sources, for example high load from river discharge.

In respect of fine sediment transport, relative contribution of residual flow and tidal asymmetry was analyzed during spring neap cycle and 24 hours tidal cycle. In general, during SW monsoon current, contribution of residual flow is more significant than tidal asymmetry in almost all observation point, except at W2J, where tidal asymmetry is relatively dominant to drive fine sediment transport. Furthermore, based spring neap analysis, different driven transport mechanisms can be divided into residual flow induced transport, combined between residual flow and tidal asymmetry and tidal asymmetry induced residual transport. Combination of residual flow and tidal asymmetry induced transport is observed at Sawabuoy and Sisterbuoy during spring tide, while residual flow induced transport occurs at other points both during spring and neap tides.

As maximum flow direction is concerned, during SW, local maximum flow direction is dominated by westward direction, which represents ebb dominant flow, except at Banyanbuoy and Sawabuoy that maximum flow direction is ebb direction.

During spring neap cycle in the NE monsoon, majority driven mechanisms of fine sediment transport is dominated by residual flow induced transport. Combination of tidal asymmetry and residual flow is observed during spring tide Sawabuoy, which is similar to transport during SW monsoon. Moreover, maximum flow velocity is dominated by westward flow, which represents ebb dominant flow.

The importance of residual flow to induce fine suspended sediment transport relative to tidal asymmetry agrees with research from Van de Kreeke and Robaczewska (1993), who

studied the importance of the residual term versus the M_2-M_4 tidal asymmetry terms. However, study from Van der Molen (2002), compared the importance of both terms for large scale san transport in the North sea and concluded that they were in the same order of magnitude and the dominance of one term to another are varied spatially. Therefore, for mixed tidal system such as the Singapore Strait, residual flow plays major role to the fine sediment transport.

6.3   Wave induced resuspension

As described in the Chapter 3, wave action in the Singapore Strait is relatively weak since the location of the strait is sheltered by surrounding island and the fetch length is relatively short. In the case of coral reefs Islands, the island provide natural barrier that reduce the wave energy. However, considering the magnitude of wave attack that can cause resuspension of fine sediment in the shallow water (h =10 Hs), then with the wave height of 40 cm, wave attack can cause resuspension to the maximum depth of 4 m. Since coral reefs island depth ranges between 0 to 15 m, then resuspension of fine sediment by wave action also should be taken into account as one of driven forces of fine sediment transport near coral reefs. However, since periodic wave height data is not available, fine sediment transport induced by wave action is not included in this report. Moreover, as wave energy is relatively low in the regions, the main physical oceanography mechanism of sediment transport is governed by tides and a seasonal net circulation. In addition to the impact of wave action to fine SSC transport, waves generated by high speed vessel are possible to cause resuspension of fine SSC along the vessel route and near surface water.

6.4   Turbidity level at coral reef islands

The nearest observation points to coral reefs islands include Rasubuoy, Banyanbuoy, Sawabuoy and Sisterbuoy and the distance of these observation points to the reef slope is between 2 to 5 kilometers. Maximum fine SSC at these observation points often exceeded 50 mg/l with the highest SSC occurs at Sawabuoy that reached 500 mg/l. Moreover, large scales of dredging and land reclamations activities become major source of fine SSC. Major dredging and land reclamation took place at Tuas Island and Jurong Island which are located approximately 12-20 km from southern coral reefs islands.

The fine suspended sediment concentration strongly relates to turbidity level around coral reef islands. Because of high turbidity level around coral reef Islands, light penetration and visibility decreasing to less than 2 m in a clear day, which is threaten the coral growth. Moreover, applying tolerance level of coral reefs to suspended sediment based on Table 4, it is clear that suspended sediment will cause major impact to the coral communities.

The driven mechanisms govern SSC variation include tidal current asymmetry that cause residual transport. The tidal currents often superimpose with monsoon currents and produce strong current that sufficient to cause resuspension of fine SSC and determine

direction of SSC transport, whether eastward or westward. Due to time slack between tidal current and SSC, turbidity events last longer than the time span of strong current. This agree with finding of Hoitink et al (2004). In some observation points, high turbidity events can occur more than weeks, for example at Sawabuoy, Rasubuoy, Sisterbuoy and Westtuas buoy, which is caused by large supply of sediment to be resuspended by strong currents.

7 Conclusions and recommendations

7.1 Conclusions

Some conclusions can be derived from this project are:

1. The location of the Singapore Strait between the Malacca Strait and the South China Sea influences the complexity of tidal and current system in the Strait. The interaction between semidiurnal tides and diurnal tides produces mixed tidal system in the strait. Tidal elevation tends to be semidiurnal while the current velocity tends to be diurnal.

2. Seasonal variation of current velocity is influenced by residual flow which generated by superimpose of tidal current and monsoon current. During NE monsoon, average residual flow ranges from 01 to 0.3 m/s with the peak of 0.8 m/s in January and dominant residual flow is westward. During SW monsoon, residual flows range from 0.1 m/s to 0.2 m/s and it is relatively random during the transition period (June-July).

3. Residual flow plays more significant role in fine sediment transport mechanism than tidal asymmetry.

    a. During NE monsoon, relative contribution of residual flow to tidal asymmetry is observed during spring at Banyanbuoy and Rasubuoy. Combined of residual flow and tidal asymmetry governing sediment transport is observed at Sawabuoy and Sisterbuoy. Tidal asymmetry induced sediment transport is found at W2J. Most of maximum flow direction is ebb dominant flow.

    b. During SW monsoon, the relative contribution of residual flow to flow asymmetry during spring and neap is observed at most of observation points, except at Sawabuoy, where combined residual flow and tidal asymmetry govern sediment transport during spring. Maximum flow direction is dominated by ebb flow (westward).

4. Sediment supply likely comes from dredging activities (seabed dredging, dumping of dredging material) and high river discharge. However, river discharge influence is still inconclusively because of data limitation (*e.g.* time series of river discharge and sediment properties analysis).

5. Wave actions resuspend sediment concentration at near surface. However, in general, wave impact does not show significant role in fine sediment transport, particularly in the depth more than 4 m.

6. Turbidity level near coral reefs Island corresponds to the fine sediment concentrations variations. High turbidity events occur at all observations points and far from optimal

level for coral growth. Moreover, high turbidity prevents light penetration to the depth of 4 m.

7.2 Recommendations

1. Comprehensive tidal harmonic analysis should be included in the further study in order to determine relative influence of interaction between different tidal constituents to tidal asymmetry and flow asymmetry.

2. Analysis on fine sediment properties is important to determine the sediment characteristic and its influence to the fine sediment transport

3. Numerical modeling of fine sediment transport by incorporating possible driven forces such as wave, tide, wind and monsoon circulation, can be used to simulate complexity of sediment transport system in the Singapore Strait.

8   References

AUBREY, D. G. & SPEER, P. E. (1985) A Study of Non-Linear Tidal Propagation in Shallow Inlet/Estuarine Systems Part I: Observations. *Estuarine, Coastal and Shelf Science,* 21**,** 185-205.

BIRD, M., CHUA, S., FIFIELD, L. K., TEH, T. S. & LAI, J. (2004) Evolution of the Sungei Buloh-Kranji Mangrove Coast, Singapore. *Applied Geography,* 24**,** 181-198.

BIRD, M. I., FIFIELD, L. K., TEH, T. S., CHANG, C. H., SHIRLAW, N. & LAMBECK, K. (2007) An Inflection in the Rate of Early Mid-Holocene Eustatic Sea-Level Rise: A New Sea-Level Curve from Singapore. *Estuarine, Coastal and Shelf Science,* 71**,** 523-536.

BIRD, M. I., PANG, W. C. & LAMBECK, K. (2006) The Age and Origin of the Straits of Singapore. *Palaeogeography, Palaeoclimatology, Palaeoecology,* 241**,** 531-538.

BOSBOOM.J & STIVE, M. J. F. (2010) Lecture Notes: Coastal Dynamic I. TU Delft.

CHAN, E., TKALICH, P., GIN, K. & OBBARD, J. (2006) The Physical Oceanography of Singapore Coastal Waters and Its Implications for Oil Spills. *The Environment in Asia Pacific Harbours.*

CHEN, M., MURALI, K., KHOO, B. C., LOU, J. & KUMAR, K. (2005) Circulation Modeling in the Strait of Singapore. *Journal of Coastal research,* 21**,** 960-972.

CHIA, L. S., KHAN, H. & CHOU, L. M. (1988) The Coastal Environmental Profile of Singapore. Singapore, ASEAN, USCRMP.

CHOU, L. M. (1994) Marine Environmental Issues of Southeast Asia:State and Devlopement. *Hydrobiologia,* 285**,** 139-150.

CHOU, L. M. (2006) Marine Habitats in One of the Worlds's Busiest Harbours. IN WOLANSKI, E. (Ed.) *The Environment in Asia Pacific Harbours.* Netherlands, Springer.

CHOU, L. M. & CHIA, L. S. (1991) The Marine Environment IN CHIA, L. S., RAHMAN, A. & TAY.D (Eds.) *The Biophysical Environment of Singapore.* Singpaore, Singapore University Press.

CHOU, L. M., TUN, K., YEEMIN, T., NIPHON, P., AMRI, A. Y., KIM, S., NYUYEN, V. L., NANOLA, C., LANE, D. & TUTI, Y. (2008) Status of Coral Reefs in Southeast Asia. *Global Coral Reefs Status 2008.*

CHOU, L. M., YU, J. Y. & LOH, T. L. (2004) Impact of Sedimentation on Soft-Bottom Benthic Communities in the Southern Islands of Singapore. *Hydrobiologia,* 515**,** 91-104.

DE JONGE, V. N. (1992) Tidal Flow and Residual Flow in the Ems Estuary. *Estuarine, Coastal and Shelf Science,* 34**,** 1-22.

DELTARES, IMARES & BOSKALIS (2008) Project Si 4.1- Report Phase 2. Delft, Deltares.

DIKOU, A. & VAN WOESIK, R. (2006) Survival under Chronic Stress from Sediment Load: Spatial Patterns of Hard Coral Communities in the Southern Islands of Singapore. *Marine Pollution Bulletin,* 52**,** 1340-1354.

DOORN-GROEN, S. M. (2007) Environmental Monitoring and Management of Reclamations Works Close to Sensitive Habitats. *Terra et Aqua,* 108**,** 3-18.

DRONKERS, J. (1986) Tidal Asymmetry and Estuarine Morphology. *Netherlands Journal of Sea Research,* 20**,** 117-131.

FABRICIUS, K. E. (2005) Effects of Terrestrial Runoff on the Ecology of Corals and Coral Reefs: Review and Synthesis. *Marine Pollution Bulletin,* 50**,** 125-146.

GOURLAY, M. R. (1994) Wave Transformation on a Coral Reef. *Coastal Engineering,* 23**,** 17-42.

GROEN, P. (1967) On the Residual Transport of Suspended Matter by an Alternating Tidal Current. *Netherlands Journal of Sea Research,* 3**,** 564-574.

HAMID, F. A. & LEE, F. (2009) The Singapore Blue Plan. Singapore, IYOR 2008.

HESP, P. A., CHANG, C. H., HILTON, M. J., CHOU, L. M. & TURNER, I. M. (1998) A First Tentative Holocene Sea Level Curve for Singapore. *Journal of Coastal research,* 14**,** 308-314.

HILTON, M. J. & CHOU, L. M. (1999) Sediment Facies of Low Energy, Mesotidal, Fringing Reef, Singapore. *Singapore journal of tropical geography,* 20**,** 111-130.

HOITINK, A. J. F. (2003) Physics of Coral Reefs Systems in a Shallow Tidal Embayment. *Faculty of geographical science.* Utrecht, Utrecht University.

HOITINK, A. J. F. (2004) Tidally-Induced Clouds of Suspended Sediment Connected to Shallow-Water Coral Reefs. *Marine Geology,* 208**,** 13-31.

HOITINK, A. J. F. & HOEKSTRA, P. (2003) Hydrodynamic Control of the Supply of Reworked Terrigenous Sediment to Coral Reefs in the Bay of Banten (Nw Java, Indonesia). *Estuarine, Coastal and Shelf Science,* 58**,** 743-755.

HOITINK, A. J. F., HOEKSTRA, P. & VAN MAREN, D. S. (2003) Flow Asymmetry Associated with Astronomical Tides: Implication for the Residual Transport of Sediment. *Journal of Geophysical Research,* 108**,** 3315.

MASSEL, S. R. (1996) *Ocean Surface Waves: Their Physics and Prediction, Vol 11 of Advanced Series on Ocean Engineering.,* World scientific Publishing Co.Pte.Ltd.

NAJAH, A., ELSHAFIE, A., KARIM, O. A. & JAFFAR, O. (2009) Prediction of Johor River Water Quality Parameters Using Artificial Neural Networks. *European journal of scientific research,* 28**,** 422-435.

NAYAR, S., GOH, B. P. L. & CHOU, L. M. (2004a) Environmental Impact of Heavy Metals from Dredged and Resuspended Sediments on Phytoplankton and Bacteria Assessed in in Situ Mesocosms. *Ecotoxicology and Environmental Safety,* 59**,** 349-369.

NAYAR, S., GOH, B. P. L. & CHOU, L. M. (2004b) The Impact of Petroleum Hydrocarbons (Diesel) on Periphyton in an Impacted Tropical Estuary Based on in Situ Microcosms. *Journal of Experimental Marine Biology and Ecology,* 302**,** 213-232.

NAZAHIJAH, R., YUSOP, Z. & ABUSTAN, I. (2007) Strom water Quality Band Pollution Loading from an Urban Residential Catchment in Johor, Malaysia. *Water science & technology,* 56**,** 1-9.

PANG, W. C. & TKALICH, P. (2003) Modeling Tidal and Monsoon Driven Currents in the Singapore Strait. *Singapore Maritime &Port Journal***,** 151-162.

POSTMA, H. (1961) Transport and Accumulation of Suspended Matter in the Dutch Wadden Sea. *Netherlands Journal of Sea Research,* 1**,** 148-180.

ROBINSON, I. S. (1983) Tidally Induced Residual Flows. IN JOHNS, B. (Ed.) *Physical Oceanography of Coastal Ans Shelft Seas.* Amsterdam, Elsevier Science Publishers.

SDWA (2010) Large Scale Sediment Transport and Turbidity in Singapore's Coastal Waters. IN NUS, D., PUB (Ed.).

STORLAZZI, C. D., FIELD, M. E., BOTHNER, M. H., PRESTO, M. K. & DRAUT, A. E. (2009) Sedimentation Processes in a Coral Reef Embayment: Hanalei Bay, Kauai. *Marine Geology,* 264**,** 140-151.

TAN, T. S., PHOON, K., K., LEE, F. H., TANAKA, H., LOCAT, J. & CHONG, P. T. (2003) A Characterisation Study of Singapore Lower Marine Clay. *Characterisation and Engineering Properties of Natural Soils.* Lisse, Swets&Zeitlinger.

VAN DE KREEKE, J. & ROBACZEWSKA, K. (1993) Tide-Induced Residual Transport of Coarse Sediment; Application to the Ems Estuary. *Netherlands Journal of Sea Research,* 31**,** 209-220.

VAN DER MOLEN, J. (2002) The Influence of Tides, Wind and Waves on the Net Sand Transport in the North Sea. *Continental Shelf Research,* 22**,** 2739-2762.

VAN MAREN, D. S., HOEKSTRA, P. & HOITINK, A. J. F. (2004) Tidal Flow Asymmetry in the Diurnal Regime: Bed-Load Transport and Morphologic Changes around the Red River Delta. *Ocean Dynamics,* 54**,** 424-434.

VAN RIJN, L. C. (1993) *Principles of Sediment Transport in Rivers, Estuaries And Coastal Seas,* The Netherlands, Aqua Publications.

WANG, Z. B. (2008) Coastal Inlet Engineering Lecture Note: Tidal Asymmetry and Morphology. Delft, TU Delft.

WINTERWERP, J. C., MANNING, A. J., MARTENS, C., DE MULDER, T. & VANLEDE, J. (2006) A Heuristic Formula for Turbulence-Induced Flocculation of Cohesive Sediment. *Estuarine, Coastal and Shelf Science,* 68**,** 195-207.

WOLANSKI, E., FABRICIUS, K., SPAGNOL, S. & BRINKMAN, R. (2005) Fine Sediment Budget on an Inner-Shelf Coral-Fringed Island, Great Barrier Reef of Australia. *Estuarine, Coastal and Shelf Science,* 65**,** 153-158.

Wolanski, E., Fabricius, K. E., Cooper, T. F. & Humphrey, C. (2008) Wet Season Fine Sediment Dynamics on the Inner Shelf of the Great Barrier Reef. *Estuarine, Coastal and Shelf Science,* 77**,** 755-762.

Wolanski, E., Ngoc Huan, N., Trong Dao, L., Huu Nhan, N. & Ngoc Thuy, N. (1996) Fine-Sediment Dynamics in the Mekong River Estuary, Vietnam. *Estuarine, Coastal and Shelf Science,* 43**,** 565-582.

Wong, P. P. (1985) Artificial Coastlines: The Example of Singapore. *Geomorph,* 57**,** 175-192.

Woolfe, K. J. & Larcombe, P. (1999) Terrigenous Sedimentation and Coral Reef Growth: A Conceptual Framework. *Marine Geology,* 155**,** 331-345.

Zhang, Q. Y. & Gin, K. Y. H. (2000) Three-Dimensional Numerical Simulation for Tidal Motion in Singapore's Coastal Waters. *Coastal Engineering,* 39**,** 71-92.

Zimmerman, J. T. F. (1980) Vorticity Transfer by Tidal Curretns over an Irregular Topography. *J.Mar Res,* 38**,** 601-630.

9   Appendices

1.   **Appendix A.**
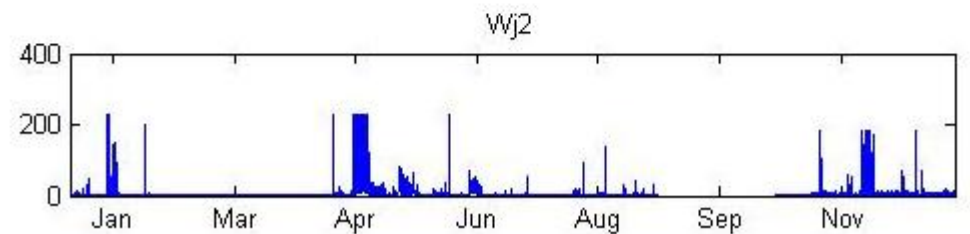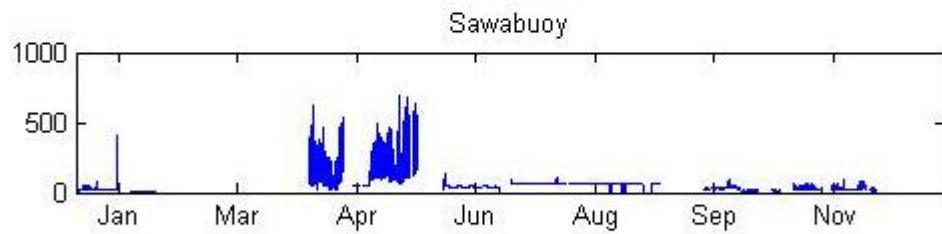   a.   **Current velocity and tide water level in July 2003**
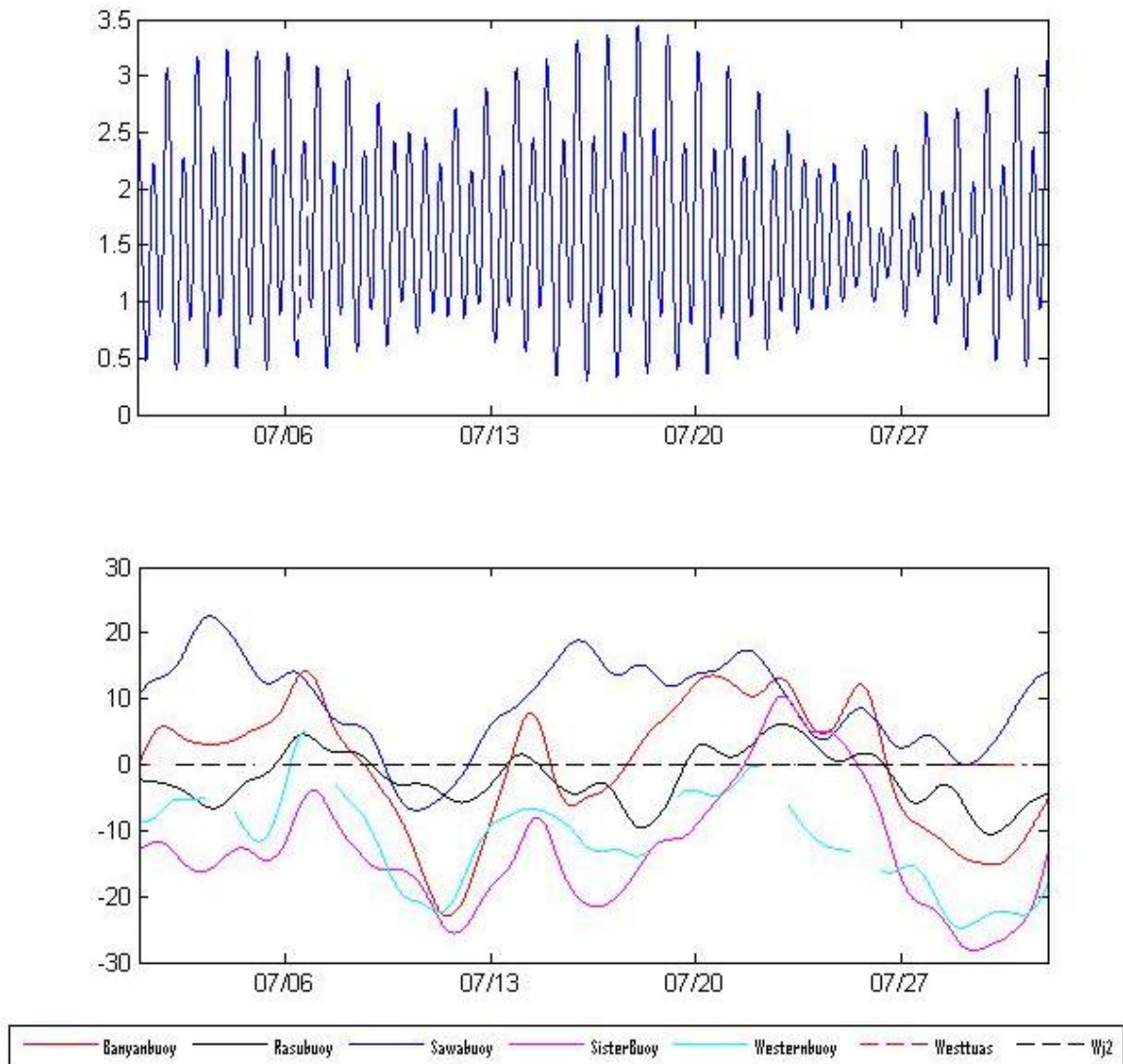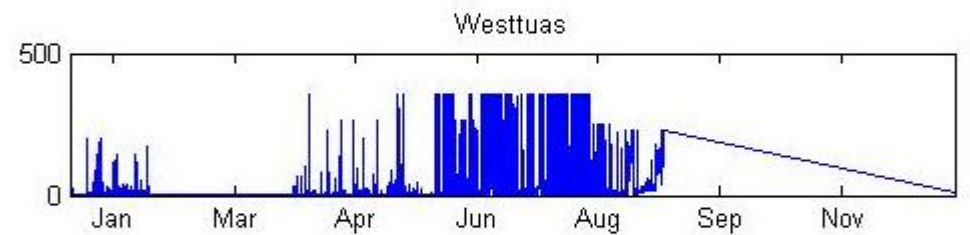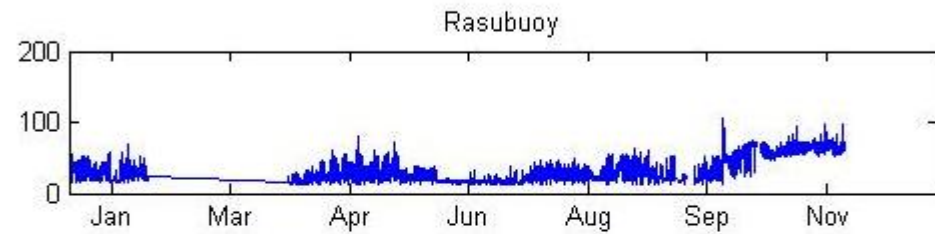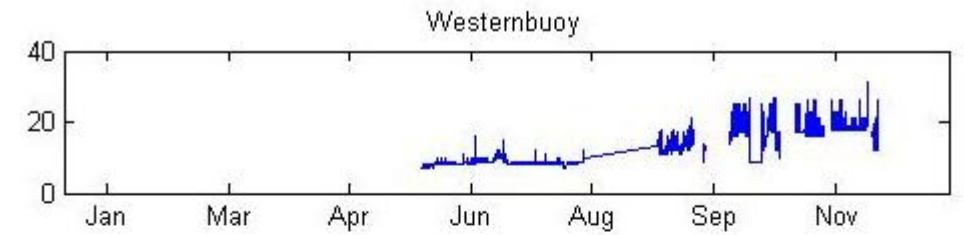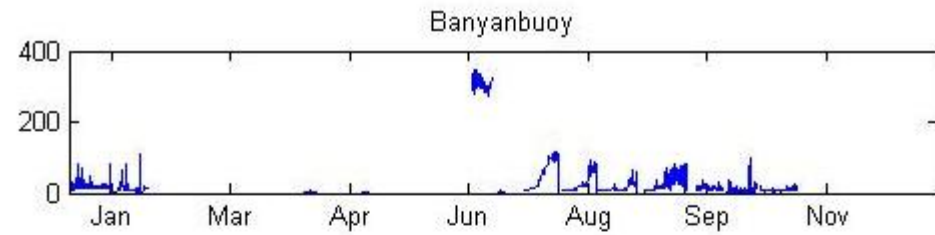
b. Current velocity and tide water level in August 2003
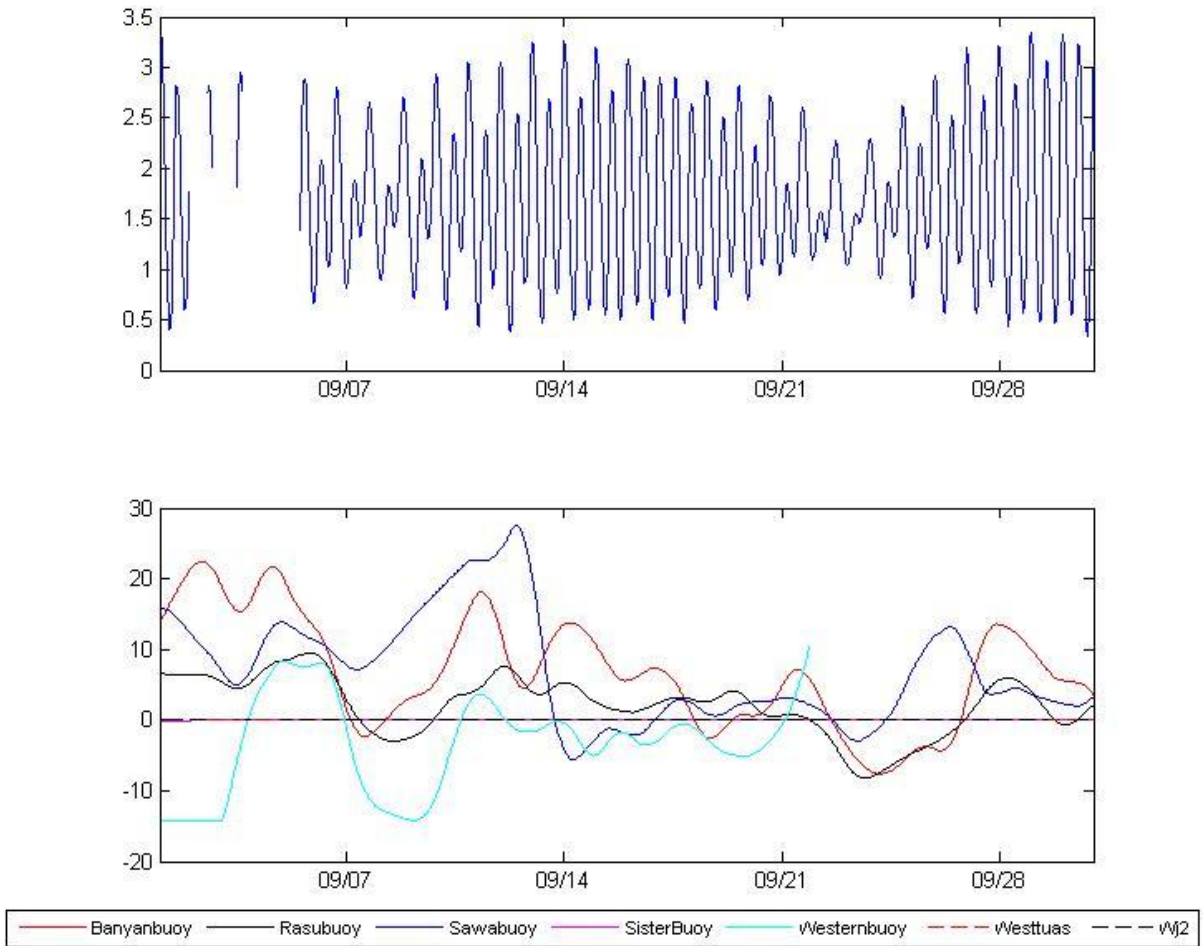
c. Current velocity and tide water level in August 2003
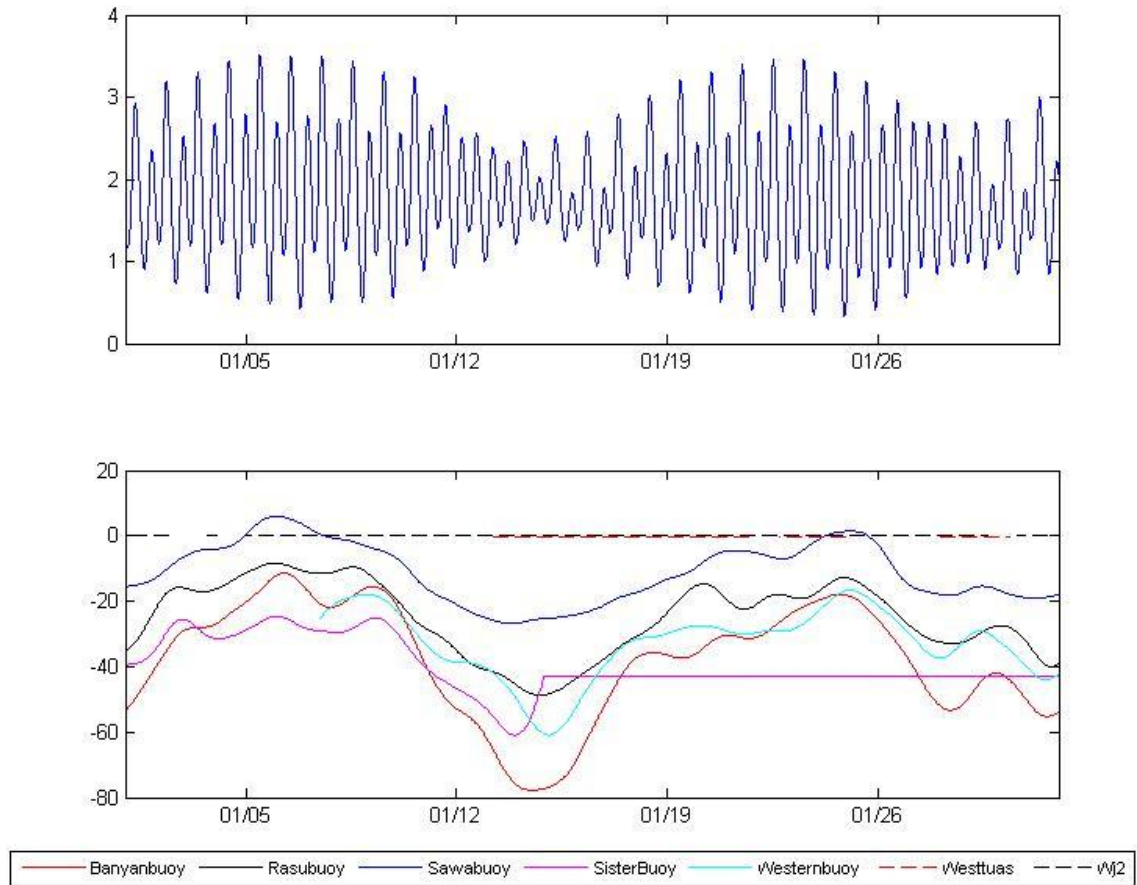
Appendix B. Suspended Sediment concentration at all observation points
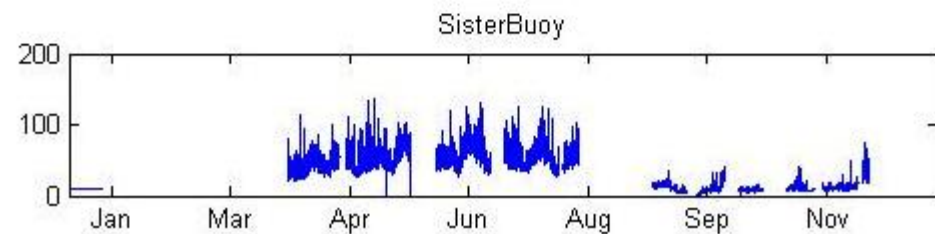
Appendix C. Current velocity data from all observation points